Demonstration of Active Combustion Control

Jeffery A. Lovett
Pratt & Whitney, East Hartford, Connecticut

Karen A. Teerlinck and Jeffrey M. Cohen
United Technologies Research Center, East Hartford, Connecticut

NASA STI Program . . . in Profile

Since its founding, NASA has been dedicated to the advancement of aeronautics and space science. The NASA Scientific and Technical Information (STI) program plays a key part in helping NASA maintain this important role.

The NASA STI Program operates under the auspices of the Agency Chief Information Officer. It collects, organizes, provides for archiving, and disseminates NASA's STI. The NASA STI program provides access to the NASA Aeronautics and Space Database and its public interface, the NASA Technical Reports Server, thus providing one of the largest collections of aeronautical and space science STI in the world. Results are published in both non-NASA channels and by NASA in the NASA STI Report Series, which includes the following report types:

- TECHNICAL PUBLICATION. Reports of completed research or a major significant phase of research that present the results of NASA programs and include extensive data or theoretical analysis. Includes compilations of significant scientific and technical data and information deemed to be of continuing reference value. NASA counterpart of peer-reviewed formal professional papers but has less stringent limitations on manuscript length and extent of graphic presentations.

- TECHNICAL MEMORANDUM. Scientific and technical findings that are preliminary or of specialized interest, e.g., quick release reports, working papers, and bibliographies that contain minimal annotation. Does not contain extensive analysis.

- CONTRACTOR REPORT. Scientific and technical findings by NASA-sponsored contractors and grantees.

- CONFERENCE PUBLICATION. Collected papers from scientific and technical conferences, symposia, seminars, or other meetings sponsored or cosponsored by NASA.

- SPECIAL PUBLICATION. Scientific, technical, or historical information from NASA programs, projects, and missions, often concerned with subjects having substantial public interest.

- TECHNICAL TRANSLATION. English-language translations of foreign scientific and technical material pertinent to NASA's mission.

Specialized services also include creating custom thesauri, building customized databases, organizing and publishing research results.

For more information about the NASA STI program, see the following:

- Access the NASA STI program home page at *http://www.sti.nasa.gov*

- E-mail your question via the Internet to *help@sti.nasa.gov*

- Fax your question to the NASA STI Help Desk at 301–621–0134

- Telephone the NASA STI Help Desk at 301–621–0390

- Write to:
  NASA Center for AeroSpace Information (CASI)
  7115 Standard Drive
  Hanover, MD 21076–1320

NASA/CR—2008-215491

Demonstration of Active Combustion Control

Jeffery A. Lovett
Pratt & Whitney, East Hartford, Connecticut

Karen A. Teerlinck and Jeffrey M. Cohen
United Technologies Research Center, East Hartford, Connecticut

National Aeronautics and
Space Administration

Glenn Research Center
Cleveland, Ohio 44135

December 2008

Acknowledgments

Level of Review: This material has been technically reviewed by NASA technical management.

Foreword

This report is the Final Contractor Report for Phase II of a NASA sponsored research program to study active combustion instability control. This work was conducted under the Turbine Engine System Technology (TEST) Contract no. NAS3–98005, and was jointly managed by the Controls and Dynamics Technology Branch and the Combustion Branch of the NASA Glenn Research Center at Lewis Field in Cleveland, Ohio. The primary objectives of the Phase II program were to apply fuel actuators and closed-loop control and to demonstrate closed-loop active combustion control of combustion instabilities using the single-nozzle rig developed in Phase I.

The NASA Task Manager for Phase II was Mr. John C. DeLaat of NASA Glenn Research Center at Lewis Field. Dr. Jeffery A. Lovett was the program manager at Pratt & Whitney. Dr. Jeffrey M. Cohen was the team leader at United Technologies Research Center. The combustion tests were conducted at the Jet Burner Test Stand, Cell no. 2, at United Technologies Research Center in East Hartford, Connecticut.

Contents

Demonstration of Active Combustion Control

Jeffery A. Lovett
Pratt & Whitney
East Hartford, Connecticut 06108

Karen A. Teerlinck and Jeffrey M. Cohen
United Technologies Research Center
East Hartford, Connecticut 06108

Summary

The primary objective of this effort was to demonstrate active control of combustion instabilities in a direct-injection gas turbine combustor that accurately simulates engine operating conditions and reproduces an engine-type instability. Most active instability control demonstrations have involved applications which use lean premixed or lean, direct combustion strategies. The subject effort was focused on a combustor with a rich/quench/lean design, which is more typical of operational aircraft engine gas turbine systems. This application presents several challenges:

(1) Liquid two-phase fuel injection
(2) Impinging, pre-filming fuel injector coupled in an air assist fuel nozzle
(3) High-frequency, moderate amplitude oscillations
(4) Limited available high-frequency actuator technology

This report documents the second phase of a two-phase effort. The first phase involved the analysis of an instability observed in a developmental aeroengine and the design of a single-nozzle test rig to replicate that phenomenon. This was successfully completed in 2001 and is documented in the Phase I report. This second phase was directed toward demonstration of active control strategies to mitigate this instability and thereby demonstrate the viability of active control for aircraft engine combustors. This involved development of high-speed actuator technology, testing and analysis of how the actuation system was integrated with the combustion system, control algorithm development and demonstration testing in the single-nozzle test rig.

A 30 percent reduction in the amplitude of the high-frequency (570 Hz) instability was achieved using actuation systems and control algorithms developed within this program. Even larger reductions were shown with a low-frequency (270 Hz) instability. This represents a unique achievement in the development and practical demonstration of active combustion control systems for gas turbine applications.

1.0 Introduction

1.1 Background

Combustion instabilities have been problematical for combustor designers since the first jet engines were developed. Combustion instability remains one of the most critical challenges today as advanced combustion systems aim for higher performance and energy release, and lower emissions. Presently, combustion instabilities are often discovered late in the development cycle and require extended and expensive empirical development tests to find a solution, often with an adverse impact on overall performance. Although the understanding of mechanisms for combustion instability has improved greatly in recent years, models and tools capable of predicting and apriori avoiding combustion instability simply do not exist. The root of the difficulty lies in the complex, highly interactive nature of combustion instabilities, and the strong nonlinearities which allow relatively subtle features to have a significant impact on the behavior. It is likely to be some time before analytical tools reach the fidelity where combustors can be designed to avoid all combustion instabilities.

A potentially powerful means of eliminating combustion instability is to actively control the oscillations using closed-loop fuel modulation. This technique requires less of a knowledge of the fundamental physical processes of unsteady combustion and relies more on the engineering development of components and control systems. This area has been a focus of extensive laboratory research activity over the past 20 years [Zinn and Neumeier, 1997]. Here a controlled fluctuating heat release is generated based on sensed oscillations in the combustor to counteract the instability. In its simplest form, the effect can be viewed as a form of interference damping. Active control methods have the potential of controlling many modes of instability over the entire operating range of the combustion system. At a minimum, active control can be used to mitigate instabilities that empirical (passive) methods are unable to eliminate. The most common method to implement active control is through fuel modulation, which then requires a fuel control valve with significant frequency bandwidth and modulation strength. The development of practical fuel actuation valves remains the crucial step in active control development.

A collaborative program was established between Pratt & Whitney, United Technologies Research Center and the NASA Glenn Research Center to demonstrate active control for aircraft engine combustor instabilities. In doing so, the viability of closed-loop, high-bandwidth control of fuel injection has been demonstrated, which could lead to advanced combustion control capabilities beyond instability control, such as mixing control and temperature pattern-factor control. The program was sponsored by the NASA Smart Efficient Components Project and managed by the Controls and Dynamics Technology Branch and the Combustion Branch at NASA Glenn. The program was executed in two phases with the aim to demonstrate active control of instabilities on an engine-scale combustor to prove the applicability of this technology for aircraft engines.

The primary objectives of the first phase of the program (executed under the Large Engine Technology Contract, Task 63A) were to identify a combustion instability experienced in an engine environment and to demonstrate that this engine instability could be replicated in a single-nozzle test rig to provide an engine-traceable test platform for combustion instability control research. A survey of Pratt & Whitney aircraft engine experience with combustion instability was conducted and a development configuration of the combustor for an advanced military engine was selected as the best candidate instability event to replicate. The frequency of the instability was 525 Hz with an amplitude of approximately 1.5 psi p-p. Evidence existed to indicate the instability was directly related to the Triwall fuel injector used in the engine. A single nozzle, axisymmetric combustor was designed based on replicating the sub-component lengths, cross-sectional area distribution, flow distribution, pressure-drop distribution and temperature distribution. The test rig developed for this purpose is illustrated in Figure 1.1 and was used for both the Phase I and present studies. Analytical models were applied to predict the acoustic resonances of this single-nozzle test rig and of the engine combustion system. The
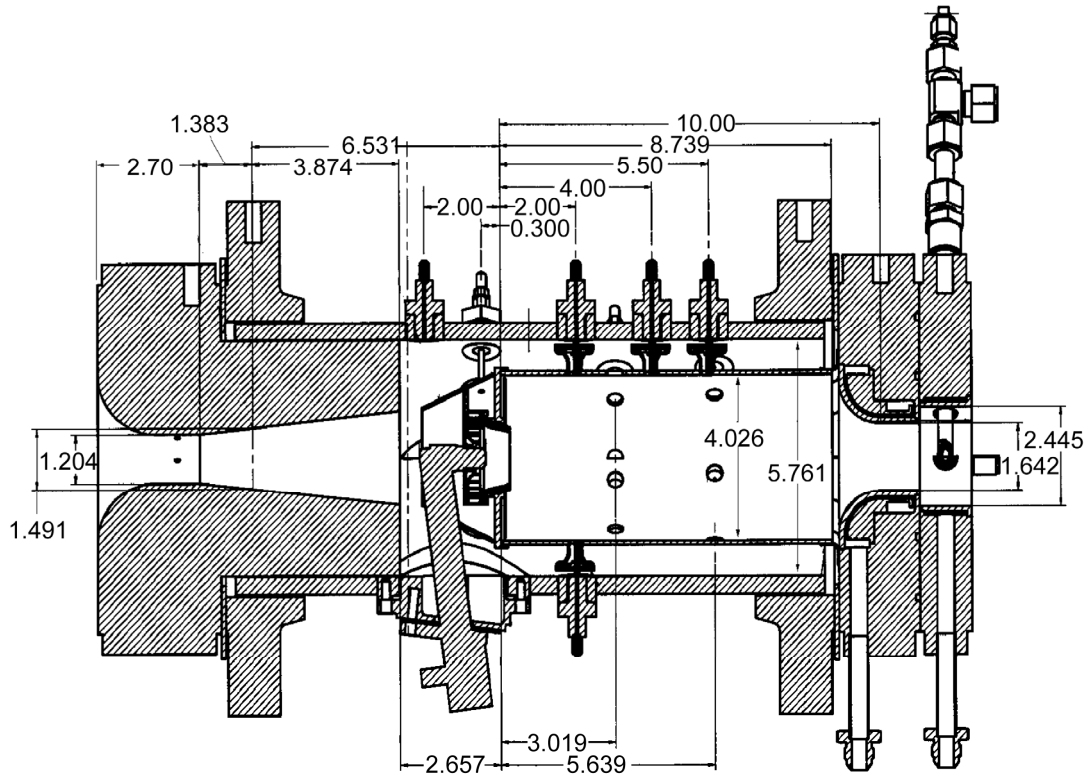
Figure 1.1.—The combustor test rig assembly.

model results confirmed that the test rig configuration and engine configuration had similar longitudinal acoustic characteristics. Parametric studies were performed to understand the influence of geometry and condition variations and the resulting rig tests demonstrated a longitudinal combustion instability at 570 Hz relative to a program goal of 525 Hz. A comparison of the engine and test rig pressure spectra is shown in Figure 1.2. The measured amplitude of the instability was approximately 0.8 psi peak-to-peak relative to a program goal of 1.5 psi peak-to-peak observed in the engine during accelerating conditions. The measured dynamic pressures at several positions in the combustor were in general agreement with the longitudinal modes predicted by 1–D modeling results for the engine and rig. Overall, this instability appeared to be consistent with the longitudinal mode observed in the engine and was concluded to be a good representation of the engine instability for the active control demonstration [Cohen, et al., 2000, DeLaat, et al., 2000]. A modification to the system geometry was also examined (upstream boundary condition moved upstream 19 in.) to perturb the system acoustics and was found to produce a substantial change in the instability behavior with very strong amplitudes measured at about 270 Hz, as shown by the pressure spectrum in Figure 1.3. These results demonstrated the direct importance that the acoustic environment plays and provided a relatively strong instability to study as well. Additional acoustic analysis was conducted under Phase II to explain this acoustic mode.

The Phase I effort successfully demonstrated that longitudinal combustion instabilities observed in an aircraft engine can be replicated by design in a single-nozzle test rig, readying a platform for the study of active combustion instability control in this Phase II effort.
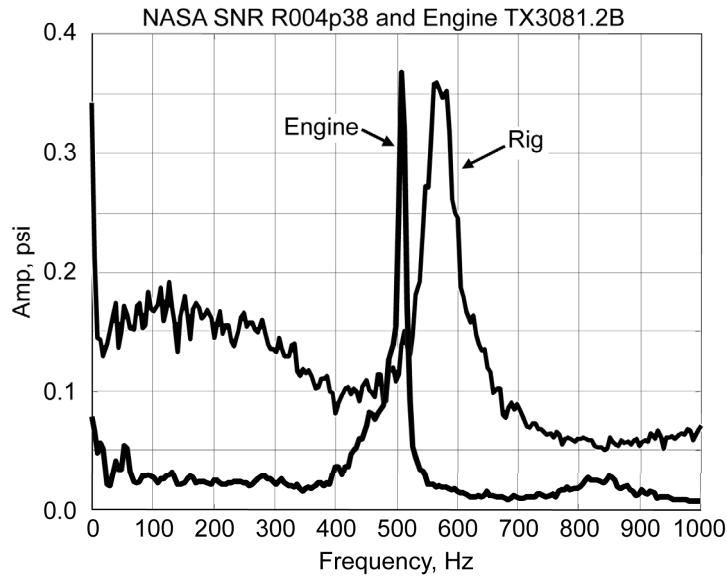
Figure 1.2.—Comparison of engine and single-nozzle combustor pressure spectra for design-point operation (combustor inlet air temperature T_3 = 770 °F, combustor inlet air pressure P_3 = 200 psia, fuel/air ratio = 0.030).
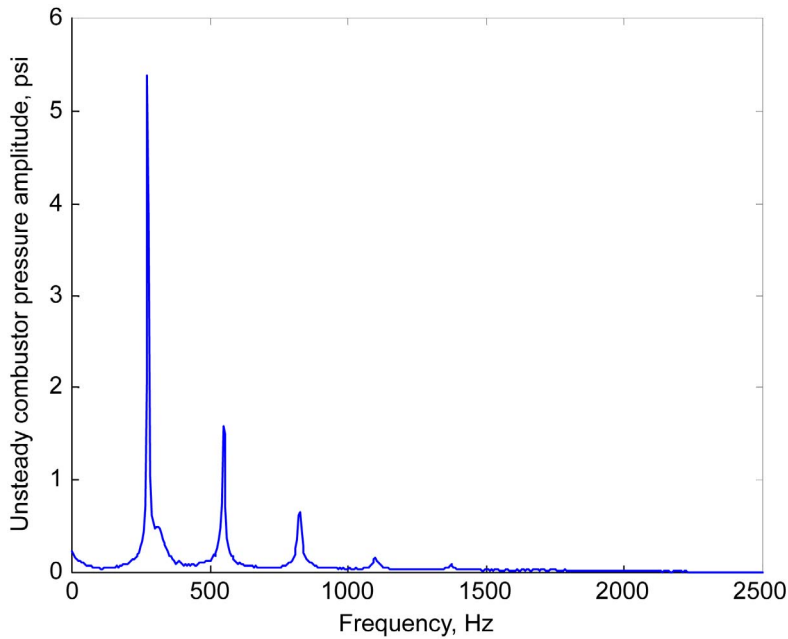
Figure 1.3.—Dynamic pressure spectrum produced with a 19 in. shift in the upstream boundary.

1.2 State of the Art

The instability mechanisms in aero engine combustors are generally believed to be either thermoacoustic or convective-acoustic in nature. Thermoacoustic instability is a classical problem - it arises when unsteady heat release couples with the resonant acoustic modes of the combustor. When the heat release fluctuations are in phase with acoustic pressure oscillations, they drive energy into the

acoustic pressure field, leading to growth in the amplitude of the instability. Convective-acoustic instability occurs when unsteady heat release generates entropy waves, which convect downstream, interacting with steep gradients in the nozzle region and generate upstream propagating acoustic waves. In either case the unsteady heat release response of the combustion process to acoustic perturbations is a key element of the instability mechanism.

Active control of instabilities is of interest partly because it can be employed without detailed understanding of the physical interactions for instabilities. Some of the related physical processes include flame dynamics, spray dynamics, fuel supply system resonances, or more subtle fluid dynamic issues such as size-biased fuel droplet transport in an acoustic field leading to grouping of droplets. Candel's group at Ecole Central was one of the first to successfully apply a combination of sensors, actuators and control algorithms to successfully suppress pressure oscillations in a laboratory combustion system [Billoud, et al., 1992]. The emphasis of the active control program at United Technologies Research Center was initiated under DARPA (Defense Advanced Research Projects Agency) sponsorship during the late 1990's using a liquid-fueled combustor [Peracchio et al., 1998; Cohen, Rey, et al. 1998; Hibshman et al., 1999]. The control approach employed was developed using reduced-order analysis in which the coupling between the non-linear heat release and the acoustic field was described by a simple time-delay expression [Peracchio and Proscia, 1998]. In recent years, progress has been made on understanding the benefits of addressing the non-linear behavior which characterizes a controlled combustion system [Banaszuk et al., 1999; Cohen and Banaszuk, 2003]. Active control has attained the highest level of development in premixed industrial combustion systems employed in stationary and marine gas turbine engines. To date, the development of appropriate heat release models remains a challenge.

1.3 Technical Approach and Program Goals

The overall goal of both the NASA and Pratt & Whitney active control programs is to demonstrate the viability of active combustion control for instability control on real gas turbine engines. The application of active control to a full-scale engine is critically dependent on the availability of suitable high-bandwidth fuel actuators and control systems that effectively mitigate the instability. Similarly, comprehensive dynamic models of the system are also needed to maximize the understanding and effectiveness of the control approach and to allow the results to be transitioned from the laboratory to an engine system. The effort described in this report included activities to address each of these critical needs and also leveraged other related activities at NASA and P&W/UTRC.

The goal of the Phase II effort described herein is to combine modeling, actuator, and control technologies to demonstrate closed-loop active control of combustion instabilities using a combustor configuration and conditions representative of aircraft engine combustors. This is an important step towards demonstrating the viability of active control and the associated components/technologies for aircraft engine applications. It is the intent of this effort, sponsored by NASA Glenn, to provide sufficient demonstration of these technologies and associated components to achieve a NASA Technology Readiness Level (TRL) of 3, defined by demonstrations at relevant conditions in a laboratory environment. The results of this effort will help support a decision to launch follow-on technology maturation and engine-system demonstration programs. This also provides a critical element in the P&W/UTRC integrated development program to address combustion instabilities in aircraft engines by addressing the application of active control to the main combustor using a representative combustor instability.

This report describes the three main activities that make up the Phase II effort. First, the activity to develop and characterize fuel actuator components is described. Second, the development of control methods and the development and use of appropriate simulations is discussed. Finally, the application of these technologies to the control of an engine-traceable combustion instability is described, and the results of this successful demonstration are provided.

2.0 Actuator Component Development

2.1 Performance Requirements

In order to first characterize the combustor response and then perform closed-loop control, three liquid fuel modulators were employed. The first actuator was a rotating valve device developed at UTRC. The second fuel modulator was a linear magnetostrictive device developed at Georgia Tech. Both these devices were capable of modulating fuel up to at least 1 kHz. The third device was a Moog valve capable of fuel modulation at several hundred Hertz. The size and rating of these valves was based on specifications for the Single-Nozzle Rig (SNR) in the UTRC Jet Burner Test Stand. Of critical importance were the fuel flow requirements through the injector and the combustor operating pressure:

Combustor operating pressure (psia)	175
Fuel flow rate (pph of liquid fuel)	360
Injection orifice flow number	110
Flow coefficient (C_d)	0.7

To provide adequate control authority, the modulating valve must have a flow number approximately equal to the injector orifice when open. When the valve is closed the flow number must be substantially lower than the injector value to ensure good modulation. The overall frequency response requirement for the valve is approximately 1 kHz based on the experience that combustion instabilities in aero-engine combustors are typically in the 400 to 600 Hz range. The required level of fuel modulation for the active control system is not well known. Based on previous experience with laboratory combustor demonstrations [Zinn and Neumeier, 1997; Cohen, et al., 1998] a modulation level of about 10 percent was expected to provide adequate control authority. It should be noted that this modulation requirement is at the injection point and must account for the attenuation characteristics of the associated plumbing along with the capabilities of the valve. Bulk fluid properties and wave dynamics have a significant effect on the final delivered modulation. As a result, it was decided that the valve should provide a modulation authority of approximately 30 percent if possible and that this could be reduced, if necessary, with the installation of a bypass line to reduce the modulation level.

2.2 Spinning-Valve Actuator

The spinning-valve design (Fig. 2.1) was based on a rotary concept rather than a conventional reciprocating-spool configuration in order to facilitate high-frequency response. The concept used a rotating drum with twelve regularly spaced holes around the circumference, which align with holes in the surrounding housing to pass flow. By minimizing the clearance between the housing and the drum, leakage was reduced when the holes in the drum and housing were not aligned. Exit holes in the housing were radially opposed to balance pressure and minimize transverse loads. A design with two exit holes was chosen for this application to balance radial pressure loads on the shaft and provide sufficient flow capacity in a reasonably sized package.

It should be noted that additional exit holes could have been built into the housing, reducing the valve size for a given flow capacity in exchange for added plumbing complexity. Additional manifold complexity can, however, introduce unexpected acoustic response characteristics.

Unlike a reciprocating device, the upper frequency limit of the spinning valve is not limited by spool inertia or power required to accelerate it. A relatively low power is required to run this device at all frequencies to overcome motor losses, shaft seal friction and limited fluid friction in the valve chamber and high frequencies can be obtained. The disadvantage of this valve is the relative size and weight of the motor. The valve is not considered appropriate for a flight application but it does provide a straightforward and reliable high-frequency fuel actuator for laboratory use.
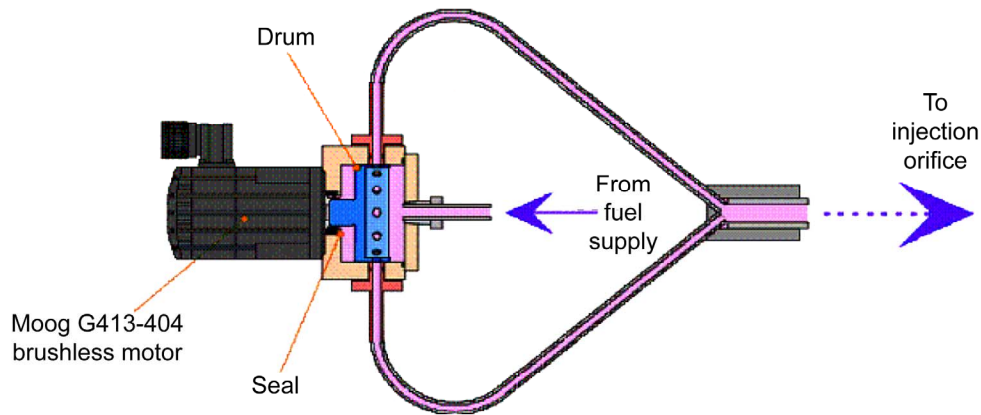
Figure 2.1.—Illustration of the spinning-valve device. The spinning valve concept uses a rotating drum with multiple holes, which align with exit holes in the case. A close tolerance is maintained to produce the maximum level of modulation and an even number of exit holes provides a pressure balance.

Two spinning-valve designs were available at UTRC. The valve employed for this program used a Moog G413-404 motor, a readily available motor capable of meeting the speed, acceleration, and precision requirements. Runout and radial clearance tolerances were better than 0.001 in., making it possible to design for clearances that minimized leakage when the valve was in a closed position. Twelve holes around the spool circumference allowed a fuel modulation frequency of 1 kHz to be reached at 5000 rpm, well within the capability of this motor.

2.2.1 Fuel Flowrate Modulation Authority

The spinning-valve system and its associated plumbing were tested in a small Jet-A flow loop with a capacity similar to that required for the single-nozzle combustor tests (~500 lbm/hr) to quantify the valve's modulation capability. The flow-loop facility is shown in Figure 2.2 and dimensions are shown in Figure 2.3. The valve was tested with a downstream orifice flow number of 100 yielding a flow capacity equal to that of the fuel nozzle. The flow loop used a 5 hp motor with a positive-displacement gear pump to drive the Jet-A flow. The fuel flowed to the test valve, through the simulated fuel nozzle, and back to a large reservoir containing about 12 gal of fuel. A bypass line upstream of the test valve could be opened to set the upstream supply pressure. The flow through this bypass line was returned to the reservoir. The fuel reservoir could be pressurized with nitrogen to simulate operation at elevated fuel system pressures (such as would be encountered during combustion tests). An accumulator or pulse damper was installed upstream of the spinning valve to reduce pressure oscillations at the valve inlet. This device was pressurized to approximately 60 percent of the operating pressure at the valve inlet and, at lower modulation levels, could dampen out almost all upstream oscillations. However, the modulation levels achieved using the spinning valve was so large that the pulse damper was less effective.

The performance metric used to evaluate this valve system was its ability to modulate the fuel flow at the point of injection, i.e., the fuel nozzle. It is difficult to directly make high-response mass-flow rate measurements and, as such, the results presented here infer flow modulation from fluctuations in pressure differential which can be reliably measured. With up- and downstream measurements close-coupled to the simulated injector, a reasonably accurate measure of flow modulation could be made. Three fuel pressure sensors (upstream of the valve, downstream of the valve, and downstream of the orifice) showed that fluctuations downstream of the injector were negligible and could be ignored and that fluctuations upstream of the valve were negligible for small levels of modulations. However, this observation did not hold for large levels of modulations and so mass flow calculations done for the high modulation cases have some uncertainty. Figure 2.4 shows a sample time trace from a pressure transducer downstream of
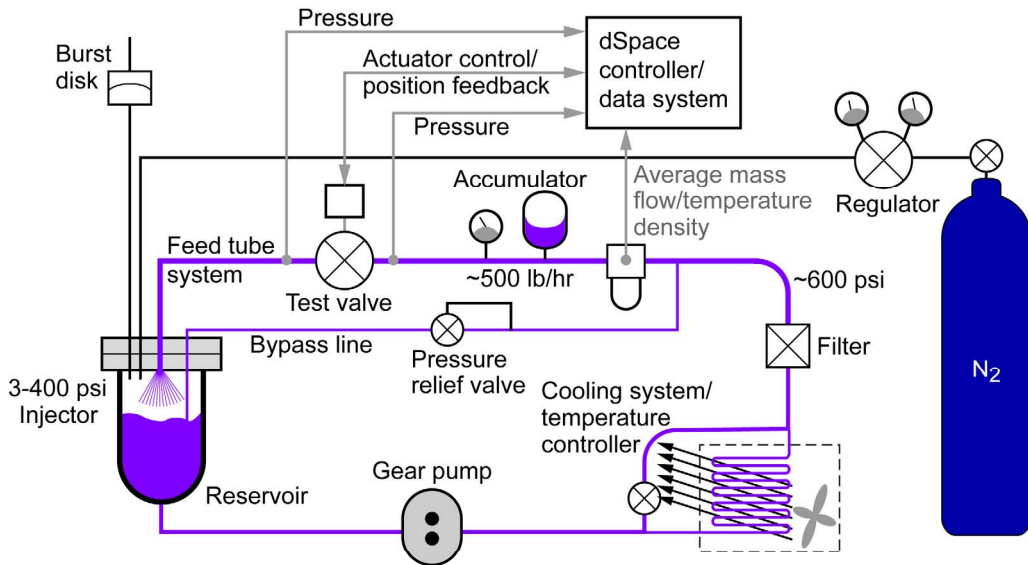
Figure 2.2.—The fuel flow loop rig for testing valve actuators at simulated elevated combustor pressures. The system allows the flow through and pressure differential across the valve to be varied. A cooling system maintains a constant temperature despite heat added from pump work at high-pressure differentials.
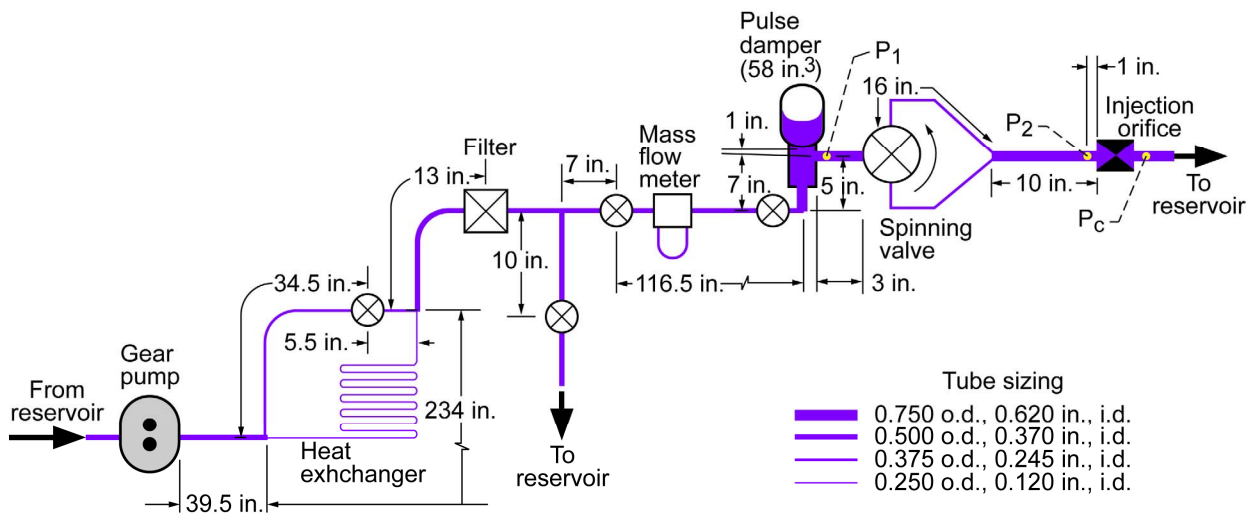

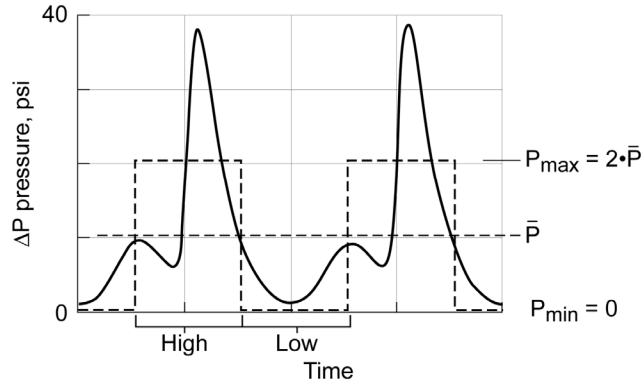Figure 2.3.—Dimensions of the fuel flow loop rig.

Figure 2.4.—Example of individual time trace of pressure used to calculate fuel flow modulation. The mean pressure was calculated and, with an assumption of a 50 percent duty cycle, the phase of maximum modulation was determined. Performance was defined as a comparison of pressure modulation against a square wave with an equivalent mean pressure.

the valve when it was running at 500 Hz. Flow modulation was inferred from pressure oscillations by a simple analysis based on the momentum equation for incompressible mass flow through an orifice in terms of the pressure differential:

$$\dot{W}_f \propto \sqrt{\Delta P} \tag{1}$$

The derivative of this equation gives the mass flow modulation with respect to time

$$\frac{\partial \dot{W}_f}{\partial t} \propto \frac{1}{\sqrt{\Delta P}} \cdot \frac{\partial(\Delta P)}{\partial t} \tag{2}$$

and normalizing this with respect to the mean mass flow (divide by equation (1)) gives

$$\frac{\partial \dot{W}_f}{\dot{W}_f} = \frac{1}{2} \cdot \frac{\partial(\Delta P)}{\Delta P} \tag{3}$$

This equation assumes that ΔP remains approximately constant ($\delta(\Delta P) \ll \Delta P$) which was not always the case for the modulation levels associated with this valve. Nonetheless, the equation was used to estimate modulation and the results compared with other methods of measurement. Despite this discrepancy, the use of pressure measurements and this correlation seem to provide reasonably accurate results, based on the results shown by Anderson et al. 1998.

2.2.2 Spinning-Valve Performance

Forced response frequency sweeps were performed using an automated dSpace routine that sweeps the valve frequency and uses a Kalman filter frequency tracker to determine the response. The speed of this process made it possible to get spectrally resolved results that were compared with those from the earlier analysis. Figure 2.5 is a sample mass flow response curve based on pressure data for the spinning valve over a range of 20 to 800 Hz. The results of the automated sweep are compared with those acquired manually and they seem to be in fairly good agreement.

Figure 2.5 presents the amplitude of fuel modulation normalized with the mean flow rate as a function of frequency. Several characteristics stand out in this response curve. The first is that the modulation levels are about 60 percent of mean flow up to 400 Hz. However, the levels did decay at the higher frequencies and a repeatable dip occurred at 500 Hz, which might be due to fuel line manifold acoustics.
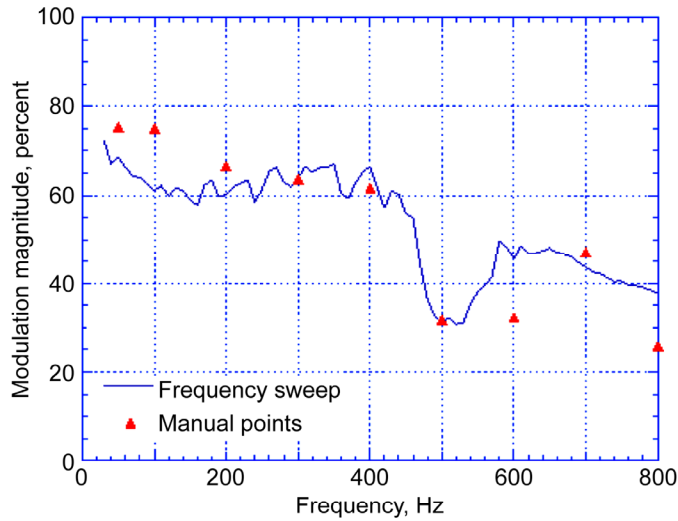
Figure 2.5.—Fuel modulation spectrum for the spinning valve. A dSpace program was used to command a motor speed, read the actual speed and measure modulation levels against an ideal sine modulation which allowed spectral sweeps to be done. The plot shows an example of valve flow modulation determined from an automated pressure sweep plotted against discrete points acquired during manual frequency forcing. Note the resonant dip around 500 Hz.
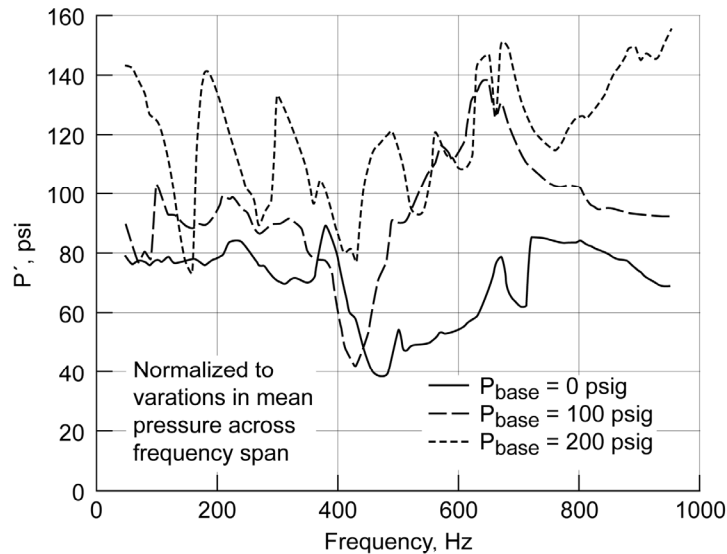

Figure 2.6.—Fuel modulation spectrum for the spinning valve. Operating the valve at elevated pressure improved the modulation level and shifts the 500 Hz resonant dip to a lower frequency. At a simulated 200 psig combustor pressure, large changes in the modulation level with frequency are believed to be the result of a resonance associated with the return tube downstream of the injection orifice.

Lengthening of the line between the valve and accumulator did show a reduction in the frequency associated with the dip in response, but because of the configuration of the accumulator plumbing, it was difficult to determine the exact line length associated with this problem. When the system was operated at higher mean pressures, the frequencies and level of attenuation were reduced. Figure 2.6 shows downstream fuel pressure (amplitude vs. frequency) as an indicator of the modulation strength as the base

pressure was changed. It was observed that elevated base pressures improved the modulation level and shifted the 500-Hz resonance to a lower frequency. It is not understood why the response changes with base pressure in this manner. Detailed acoustic analysis of the fuel system may provide a physical understanding of these behaviors. Note that Figure 2.6 shows only the modulation pressure amplitude measured downstream of the valve and not the mass flow rate amplitude per second.

From these open-loop tests in the fuel flow-loop facility it was seen that the spinning valve can generate considerable mass flow modulation capability up to frequencies approaching 1 kHz.

2.2.3 Modulation Effects on Spray Characteristics

The fuel spray atomization processes can influence the ultimate effectiveness of fuel modulation on the combustion processes with active control. For example, if the spray processes smear-out the fuel modulation the control authority of the fuel modulation could be substantially reduced. To examine this influence, the spinning valve was installed in a spray rig shown schematically in Figure 2.7. In this facility, the fuel nozzle is used to generate a fuel spray in ambient air so that the spray characteristics could be examined. Air flow was provided to simulate the flow environment that is particularly important for air blast or air-assist nozzles such as used in the present combustor.

Initial measurements were acquired with strobe photography used to "freeze" the fuel jet exiting a single orifice with a flow number 110 at a mean flow of 360 lbm/hr to test the technique and understand the basic way that the fuel jet processes the modulation. Figure 2.8 shows sample images acquired at frequencies up to 1 kHz and significant modulation of the fuel is apparent in each case. Similar images were acquired with the actual fuel injector to be used in the test rig but without the air filmer, swirler and shear airflow (Fig. 2.9). This device has six orifices with a total flow number of 110, which generate fuel streams that would otherwise impinge on a filmer-wall of the swirler so that the airflow can strip the fuel off into a fine mist. The images in Figure 2.8 again show significant modulation at the two extremes of the frequency spectrum of interest (100 and 1000 Hz) indicating that fuel modulation is not destroyed by the fuel injector configuration details or the ensuing fuel spray processes.

A semi-quantitative analysis of these images was developed to provide a measure of flow modulation effectiveness, as described in Figure 2.10. The images of each stream were separated and processed to enhance the differing intensities between the liquid fuel and surrounding air. The image intensity was then thresholded and compressed to one bit to identify the location of liquid in the stream. The total number of pixels containing liquid was summed at each axial location along the stream to determine the axial distribution of fuel as shown in the plot on the right of the figure. A correction was made for the fact that the stream is actually a 3–D, roughly axisymmetric structure and the level of modulation was then determined.
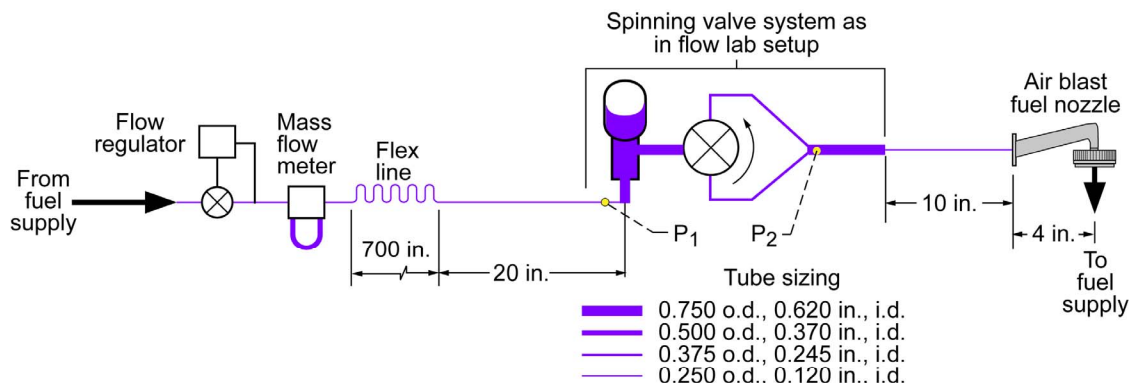

Figure 2.7.—Schematic of the spray rig used to investigate the dynamic spray effects of fuel modulation. The spray rig is an open loop system that sprays into a 1 atm environment. This provides the ability to simulate combustor primary airflow and to monitor and measure spray patterns and spray pattern modulation.

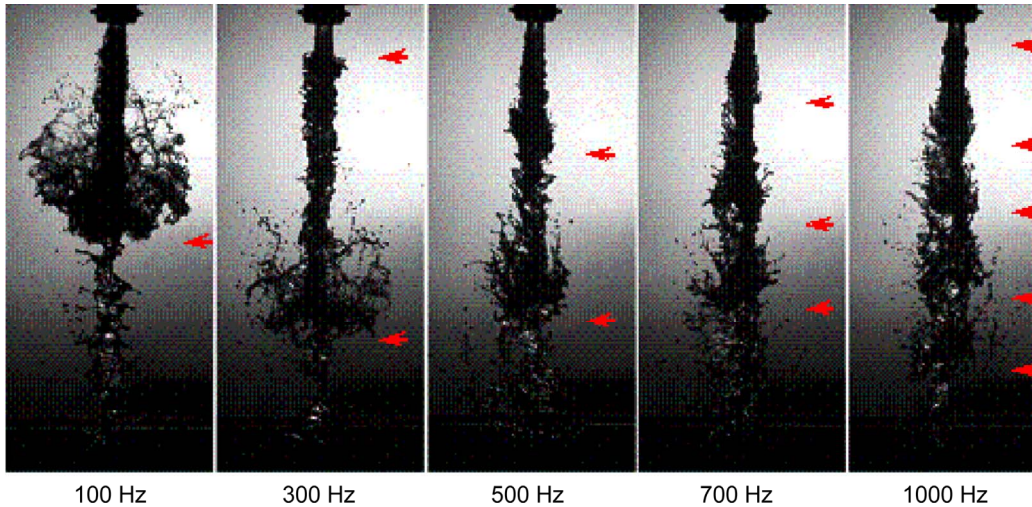100 Hz   300 Hz   500 Hz   700 Hz   1000 Hz

Figure 2.8.—Images of a fuel jet observed in the spray rig when modulating fuel flow with the
spinning valve. Flow is about 300 pph through an orifice with a flow number of 110. Significant
modulation is observed at the highest frequency, 1 kHz. The arrows point to features in the
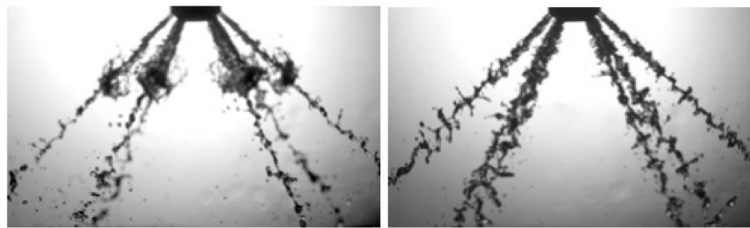flow thought to be associated with fuel modulation cycles.

Figure 2.9.—Images of the Fuel Jets from the Rig Fuel Injector. The photos
show modulation at 100 and 1000 Hz without the swirler or airflow.

Spray Image ⟶ Enhanced Image ⟶ Discrete Image ⟶ Axial volume distribution
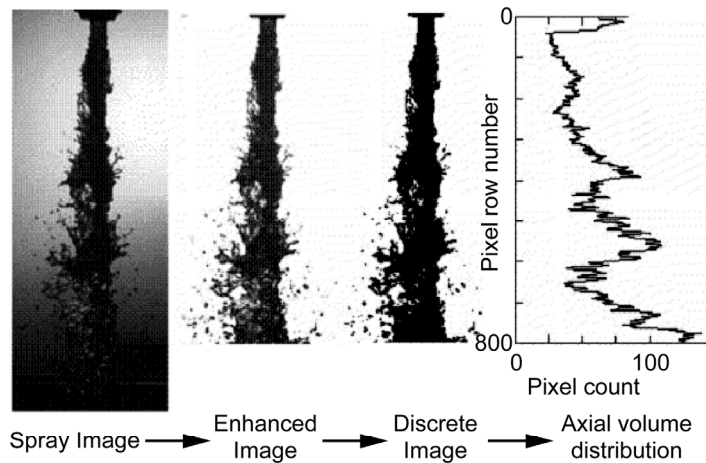
Figure 2.10.—Spray Image Analysis Process. The spray stream is enhanced
to clearly identify liquid and the image is converted to a bit map. The number
of pixels containing liquid is summed along lines perpendicular to the flow
axis to get the instantaneous axial distribution of fuel. A radial correction is
applied to determine cross sectional area and the level of axial modulation
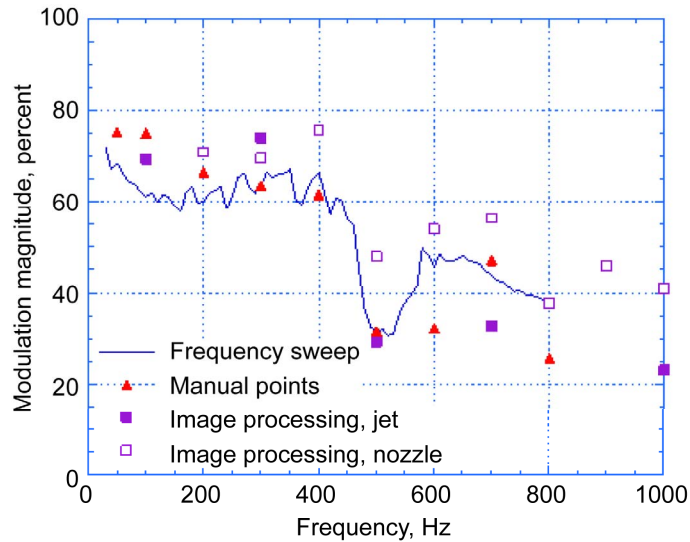is estimated.

Figure 2.11.—Modulation spectrum deduced from images
compared to spectrum from pressure measurement.

Note that a number of potential errors could occur with the analysis of the images. The assumption of an axisymmetric stream is not exactly correct. Thin regions of liquid (the lower left side of the stream in Figure 2.10), when processed, appear as air, introducing an error. Also droplets transmit light through their centers, making the most fuel-dense parts appear to be air in the processed image. In contrast, a concentrated mist can appear dark despite the relatively small amount of fuel it might contain. Notwithstanding these issues, Figure 2.11 shows the analysis results for the single stream and six-orifice nozzle images plotted against the original pressure-based data and they are in excellent agreement with the relative characteristics of the modulation spectrum implying that the technique is generally valid, and that the pressure-based modulation measurement is manifested in the fuel spray behavior.

With a level of confidence established in pressure-based flow modulation measurements, the valve/injector system was returned to the flow lab for further testing and evaluation in the closed loop flow. Modifications to the manifold configuration were made in an attempt to improve the actuator authority. The feed tube systems were modified as shown in Figure 2.12 and response data were acquired to determine the effect on system performance. A longer inlet tube between the valve and the accumulator resulted in a slight shift of the 500 Hz attenuation to a lower frequency; again suggesting that this is a Helmholtz resonator associated with the mass of fuel between the accumulator and valve and with the spring constant of the fluid in the large valve volume.

Replacing the long feed manifold between the valve and injection orifice yielded a much more significant increase in performance, however. Response at higher frequencies approximately doubled resulting in a nearly flat response except for the 500 Hz resonance. This cannot be accounted for just in terms of differing lengths between the two manifolds. It is likely that the welded "Y" junction of the original manifold contained air pockets that would not clear and provided significant frequency-dependent damping which resulted in attenuation at higher frequencies.
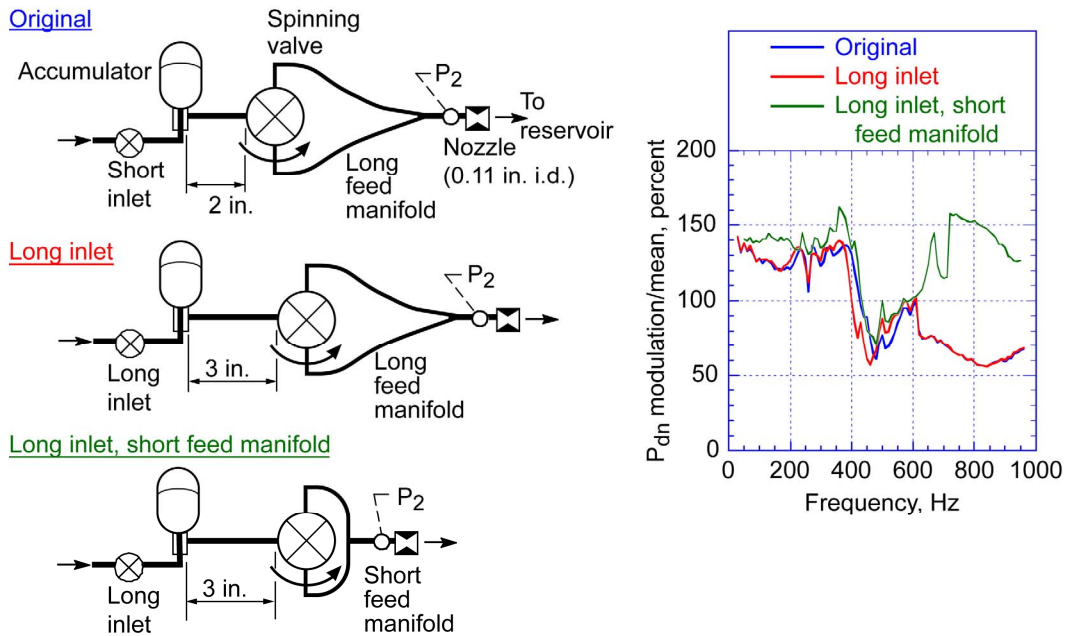
Figure 2.12.—Modulation spectrum measured with various upstream tubing lengths.

The next study conducted in the UTRC spray facility focused on documenting the fuel concentration modulation which results after the modulated fuel source is processed by the fuel injector system with the swirling air stream present. Attenuation of a laser beam passing through the spray was used as a means to measure the temporal modulation of the fuel spray. Results from these measurements are shown in Figure 2.13 and indicate the resultant fuel modulation strength near 575 Hz exiting the fuel injector with the air stream present is roughly 4 percent, indicating an attenuation of approximately 8:1 from the air-atomization process. Also, the narrow-band dip of attenuated response in the modulated fuel pressure was still present near 500 Hz. Modifications of the feed pipe length into the valve and the length of the exit plumbing were attempted to eliminate this. However, pressure measurements indicated that the dip was largely unaffected, but that the modulation strength at high frequency could be affected by the tubing lengths.

Measurements were made with the fuel injector inserted farther into the swirler, so as to cause the fuel jets to miss the filmer surface to indicate the contribution of the filming process on the modulation reductions observed in the laser attenuation measurements. Figure 2.14 shows that the fuel modulation strength is roughly doubled with the filming process removed, indicating that much of the fuel modulation attenuation is related to the filming-type atomizer. These tests established that at least qualitatively the final resultant fuel modulation strength using the spinning-valve was about 4 percent at the 570 Hz frequency. It was decided to go forward with the 4 percent modulation strength (with the fuel nozzle and swirler in their normal locations) because of the relevance of the fuel injector and instability traceability to engine experience.

An alternate fuel modulation configuration was also attempted with the spinning valve. In this alternate configuration, the pilot (primary) fuel flow was modulated rather than the main (secondary) flow. To accommodate the much smaller flow number of the pilot, the spinning-valve was placed in an additional return line just prior to the fuel nozzle. Perhaps due to the small pilot flow number and/or the additional feed system complexity and its acoustic resonances, this configuration did not seem to be particularly effective and was not pursued further.
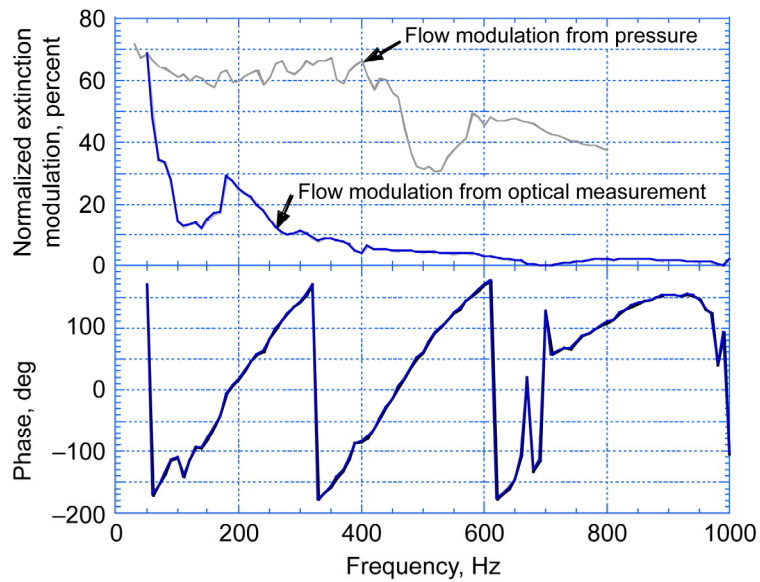
Figure 2.13.—Fuel modulation strength spectrum with air flow present compared to spectrum from fuel pressure measurement.
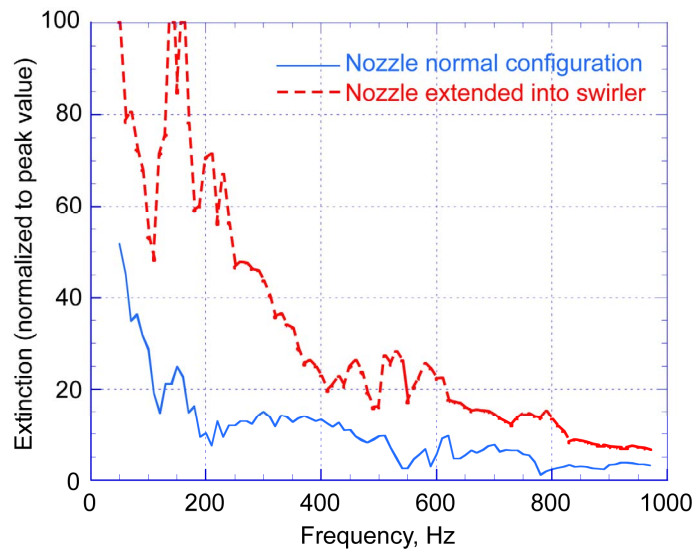

Figure 2.14.—Modulation spectrum with air flow present for two injector positions.

2.3 Georgia Tech Valve

The Georgia Tech (GT) valve, shown in Figure 2.15, is a proprietary magnetostrictive device with a large flow capacity and a very high frequency response that was developed at Georgia Tech. Because the magnetostrictive motion of the electrical material is small, the device is 18 in. long to give the stack sufficient displacement to modulate the flow. Thermal growth effects during the operation of the valve are on the order of the magnetostrictive displacement so a means of controlling mean (steady-state) flow was required. As a result, a cam system was built into the design to maintain a mean flow area for the valve while it is operating. This is done by including a low-frequency flow meter with the system and using the cam to adjust and maintain the measured mean flow.

A coarse manual adjustment on the valve (knurled knob) allows the operator to set the mean valve performance for a given flow requirement. The cam control system is then used to maintain the mean flow around that initial mean flow condition. It was found that when this was set up initially, thermal expansion of the valve due to steady operation would move the operating point beyond the range of controllability by the cam. A second manual adjustment was required after the valve had warmed up to reset it within a controllable range. The setup procedures were modified to set the course adjustment at the end of the cam travel rather than the mid-point. This allowed more cam movement to accommodate the thermal expansion and eliminated the second manual adjustment.

The controller could be operated in two modes. The first was "cam control" where the cam was maintained at an operator set point. The second was "flow control" mode where the cam was automatically adjusted to maintain a preset flow rate. The latter was proven to be the only effective way of operating the valve given the thermal changes with the valve during operation. In this mode, continual changes in system operation caused by thermal expansion and contraction were compensated for, assuring that a mean flow was maintained and that a consistent level of modulation was produced.
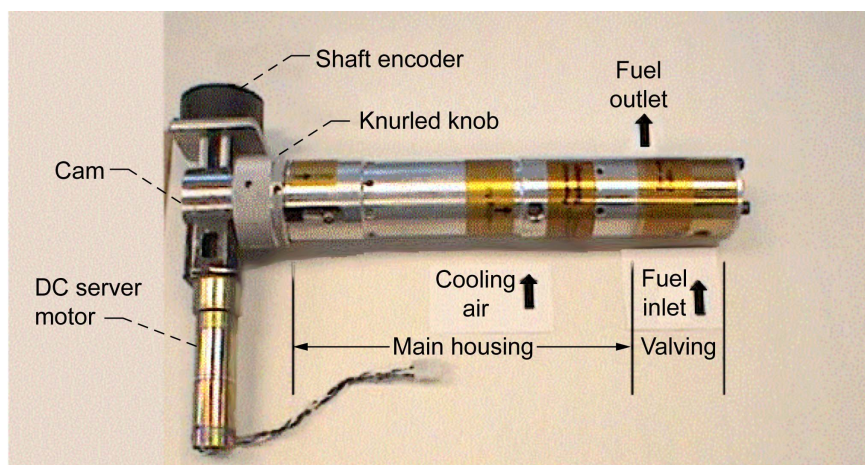

Figure 2.15.—Photograph of the Georgia Tech high-frequency magnetostrictive valve. The drive for the internal cam is shown on the left. The system also includes a flow meter and a control box.

2.3.1 Fuel Flowrate Modulation Authority

Prior to installing the valve in the single-nozzle rig, it was tested in the liquid flow-loop bench at UTRC in the configuration shown in Figure 2.16. This geometry was quite similar to that used in the combustor rig except that the fuel nozzle was replicated by a short length of tubing and an injection orifice with equivalent flow number of 125.

A sample bottle was installed in a side branch downstream of the injection orifice to reduce the oscillations observed at that point in the flow. This region represents the combustor in the real system and ideally should not have fluctuations in response to the fuel flow alone. The installation of the sample bottle accumulator was partially effective but it did not eliminate the downstream modulation, especially at higher frequencies.

Figure 2.17 shows example modulation spectra of the pressure response of the valve and feed tube system at the measurement points indicated in Figure 2.16. Pressure oscillations upstream of the GT valve were damped fairly effectively by the accumulator. Very strong modulation was observed at P_2, just downstream of the valve. There is a significant difference in the responses of P_2 and P_3, two transducers separated by only about 10 in. of tubing. The responses of the two transducers on either side of the orifice at P_3 and P_4 are quite similar. This is the result of the effective orifice cross-section (0.12 in.) being only slightly smaller than that of the tubing inner diameter (0.13 in.), introducing only minimal impedance to the system. The P_2/P_3 differences are probably due primarily to wave dynamic effects, further indicating the need for an accurate method of modeling the system dynamics.
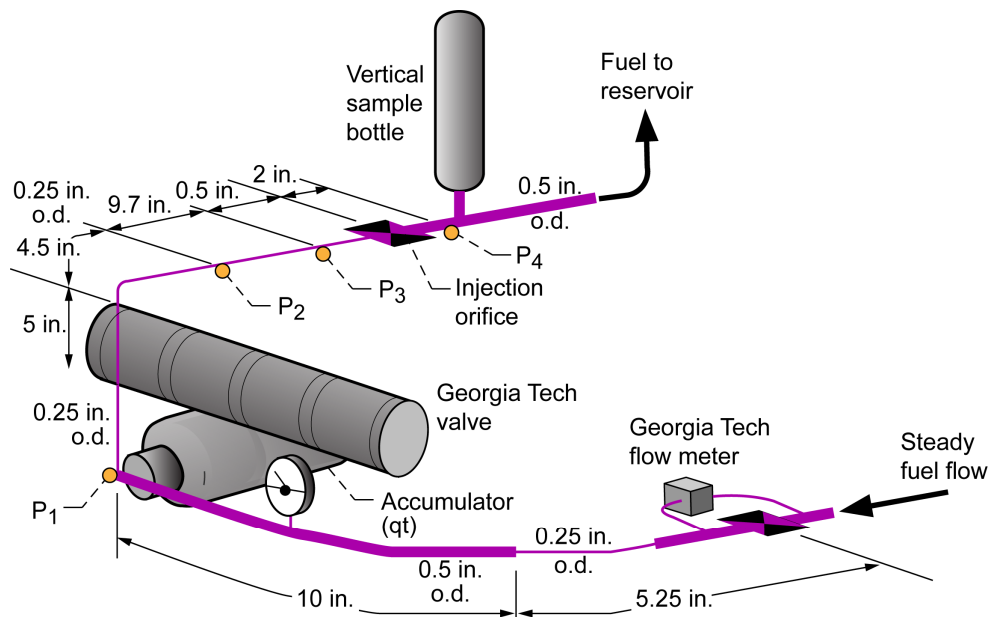

Figure 2.16.—Georgia Tech plumbing for initial flow bench tests. The injection orifice flow number was 125.
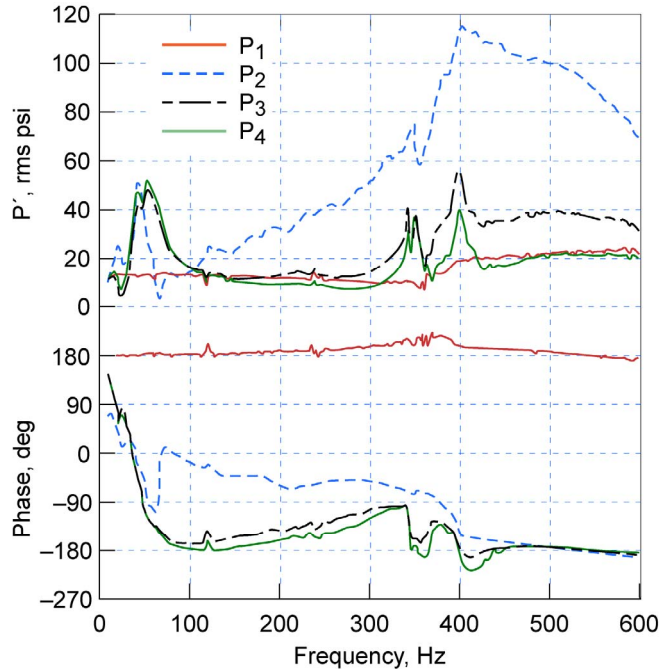
Figure 2.17.—Response performance for the Georgia Tech valve and plumbing system. Note that although P_2 and P_3 are located very near one another, their responses are quite different.
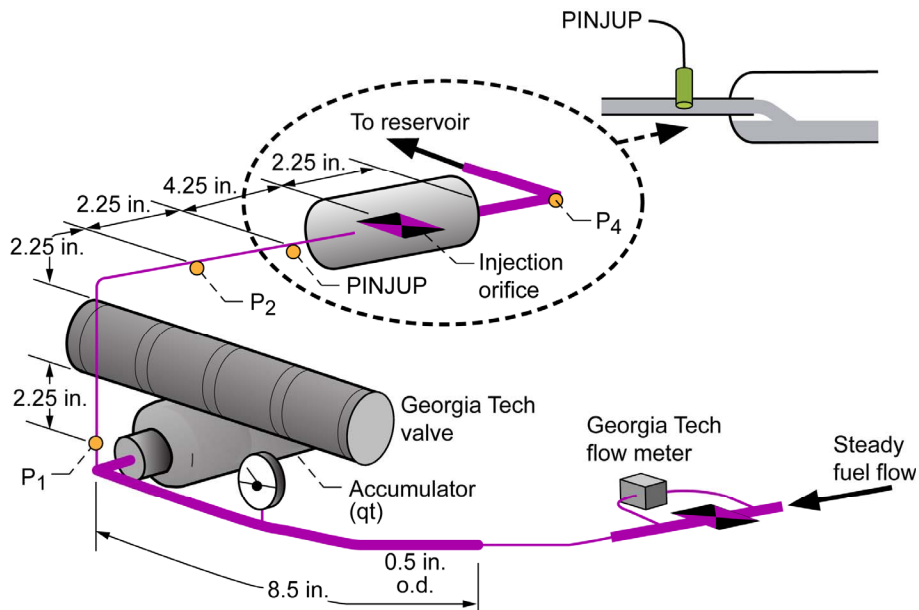

Figure 2.18.—Modified plumbing arrangement used with the Georgia Tech valve.

Plumbing modifications were made to the flow-loop rig in an attempt to reduce the oscillations observed downstream of the injection orifice. Figure 2.18 shows how the system was reconfigured with the sample bottle installed into the fuel line downstream of the injection orifice which was altered so that the fuel actually dumped into the vessel simulating the combustor. From here the fuel flowed down into the facility accumulator before being drawn into the circulating pump. A sample pressure response acquired with the modified system charged to 50 psig is shown in Figure 2.19. The plot indicates that the oscillations downstream of the orifice were greatly reduced.
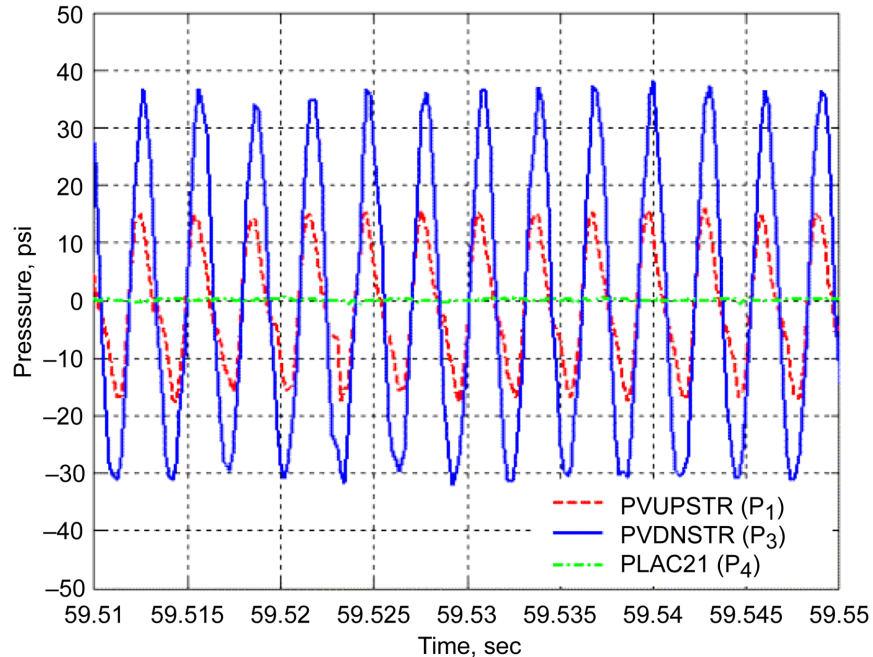
Figure 2.19.—Dynamic pressure response at 300 Hz for the modified plumbing arrangement. Oscillations in simulated combustor (green dashed-dotted line) are greatly reduced over the previous installation. PINJUP (P_3) was not recorded during this test.

After gaining more familiarity with the valve operation and working through some electrical and mechanical issues, the valve modulation performance was documented at two different operating conditions simulating the medium and high power conditions of the single-nozzle rig. Figure 2.20 shows typical swept sine results measured downstream of the modulating valve (P_2) with the system pressure (simulated P_4) charged to 95 and 160 psig, respectively, and the valve command input set to 1.0 V. These results differed from those NASA obtained [DeLaat and Chang, 2003]. NASA showed better response at the high frequencies. This left some question as to the true authority the valve could obtain when modulating the fuel into a combustor. However, as will be shown later in this report, the valve had sufficient authority for instability suppression.

2.4 Moog DDV Valve

A Moog Direct Drive Valve (DDV) was also available at UTRC and capable of providing proportional flow control with mid-frequency response. This valve could potentially be used to implement control with a variable modulation amplitude to examine the influence of control gain on closed-loop control effectiveness. The valve was installed in the flow loop rig and its frequency response was characterized. Figure 2.21 shows the pressure response measured using the Moog DDV valve which demonstrated a fairly sharp response at 300 Hz indicating that a system resonance was present with the valve system and the representative rig plumbing.
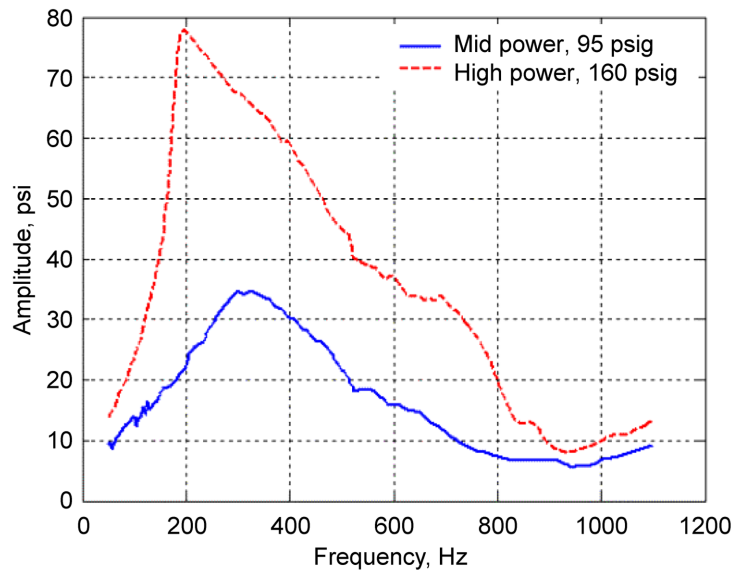
Figure 2.20.—Typical modulation spectra for the Georgia Tech valve for mid (solid blue) and high power (dashed red) conditions.
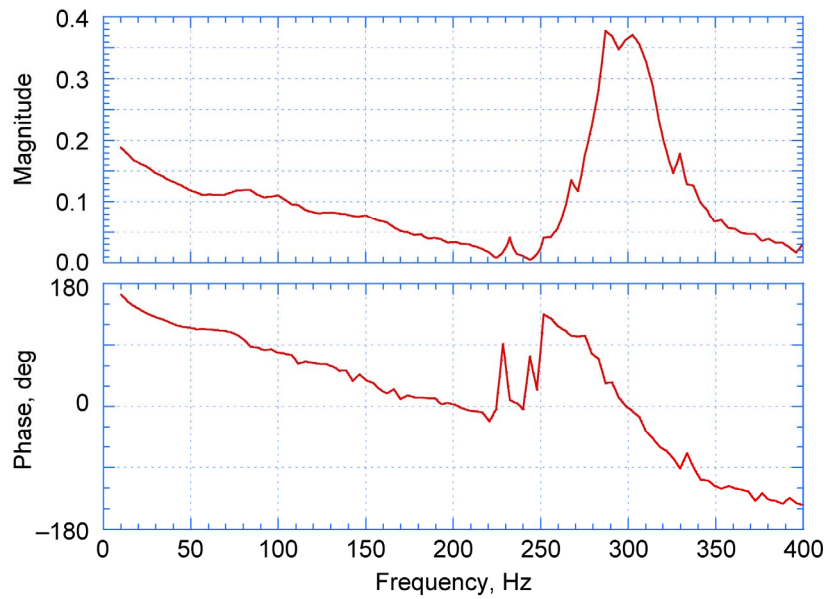

Figure 2.21.—Modulation spectra measured with the Moog DDV Valve.

3.0 Control Simulation and Development

3.1 Acoustic Analysis of Rig Acoustic Modes

The basic rig configuration developed to simulate the 525 Hz engine longitudinal acoustic mode was shown in Figure 1.1. The observed instability frequency in the test rig was 570 Hz. The 1–D standing wave acoustic tool (SWAT) was used during Phase I to understand the acoustic mode shape in the test rig. Testing during Phase I also showed that a strong 275 Hz was generated in the test rig when a 19 in. extension was installed to move the acoustic boundary at the choked venturi upstream. Acoustic analysis with the SWAT code was conducted to explain this behavior.

The original acoustic model included an inertia term for the swirler acoustic impedance related to the length of the swirler passages. With this assumption, the SWAT prediction for the baseline acoustic resonance was in excess of 600 Hz. The acoustic solution was strongly dependent on this inertance term because the acoustic velocity is high within the swirler/dome section. Considering the additional length associated with the annular passage in the fuel nozzle beyond the swirler vanes themselves, the inertia term was increased to match the observed 570 Hz frequency as an empirical calibration for this unknown term. The predicted pressure spectrum for the baseline case is shown in Figure 3.1. The amplitude shown is the relative magnitude of the acoustic gain which is proportional to the inverse of the determinate of the system. The figure shows that the 570 Hz mode is the first longitudinal standing-wave resonance as concluded earlier. With this calibration, the 19 in. upstream extension was added to the model and the predicted first longitudinal mode is shown in Figure 3.2. The geometry simulated is shown in the figure at the upper left and the acoustic response at the upper right. The 275 Hz frequency is now very accurately predicted. The mode shape, as indicated by the profiles of time varying pressure (p') and velocity (u'), shows that this configuration supports a half-wave resonance between the two choked boundaries and that the upstream extension presents a well tuned quarter-wave upstream coupled to a quarter-wave downstream. This optimized length would therefore result in a relatively high acoustic gain for this mode consistent with the relatively high levels of instability that were observed when the rig was configured for 275 Hz as shown in Figure 1.3.

3.2 Spinning Valve Control Method

A phase-shifting control algorithm was designed to suppress the 275 Hz instability with the spinning valve actuator. While the spinning valve actuator was initially designed only for forced-response testing, an effort was initiated to design a closed-loop control system around it since the valve was successful in generating high modulation strength at frequencies compatible with the low frequency rig mode. The phase-shifting controller is one of the simplest control algorithms and has been used successfully in the past for suppressing combustion instabilities [Zinn and Neumeier, 1997].

In this scheme, the main harmonic of the combustor pressure signal near the instability frequency (~280 Hz) was extracted with a filter, scaled by a control gain and shifted by a control phase which was then sent to the secondary fuel modulation actuator as the driving control signal. A modified form of an Extended Kalman Filter (EKF) based Frequency Tracking Algorithm proposed by [LaScala, 1994] was used to construct the phase shifted control signal.

A disadvantage of both a fixed-gain observer-based and delay-based phase-shifting controller is that the band-pass filters involved in these implementations are nominally fixed. If the frequency of the pressure oscillations varies over a large interval for a narrow band-pass filter, the filtered signal will be significantly attenuated and the control signal will be dominated by noise. Widening the filter bandwidth prevents attenuation of the pressure signal, but more noise is accepted. More dynamical modes can then affect the actuator action, and destabilization of these modes is possible.
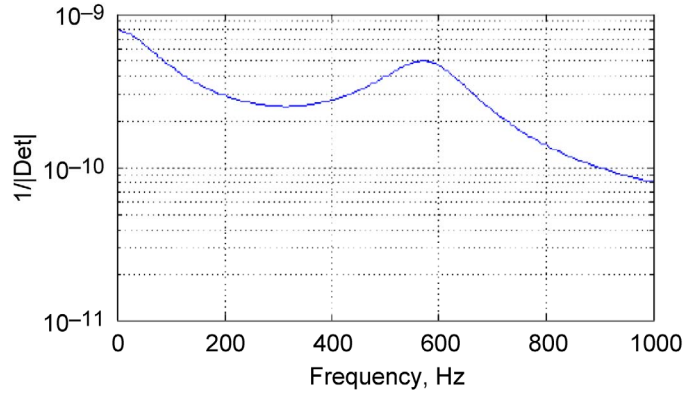
Figure 3.1.—Acoustic resonance spectrum prediction with the swirler impedance calibrated for 570 Hz.
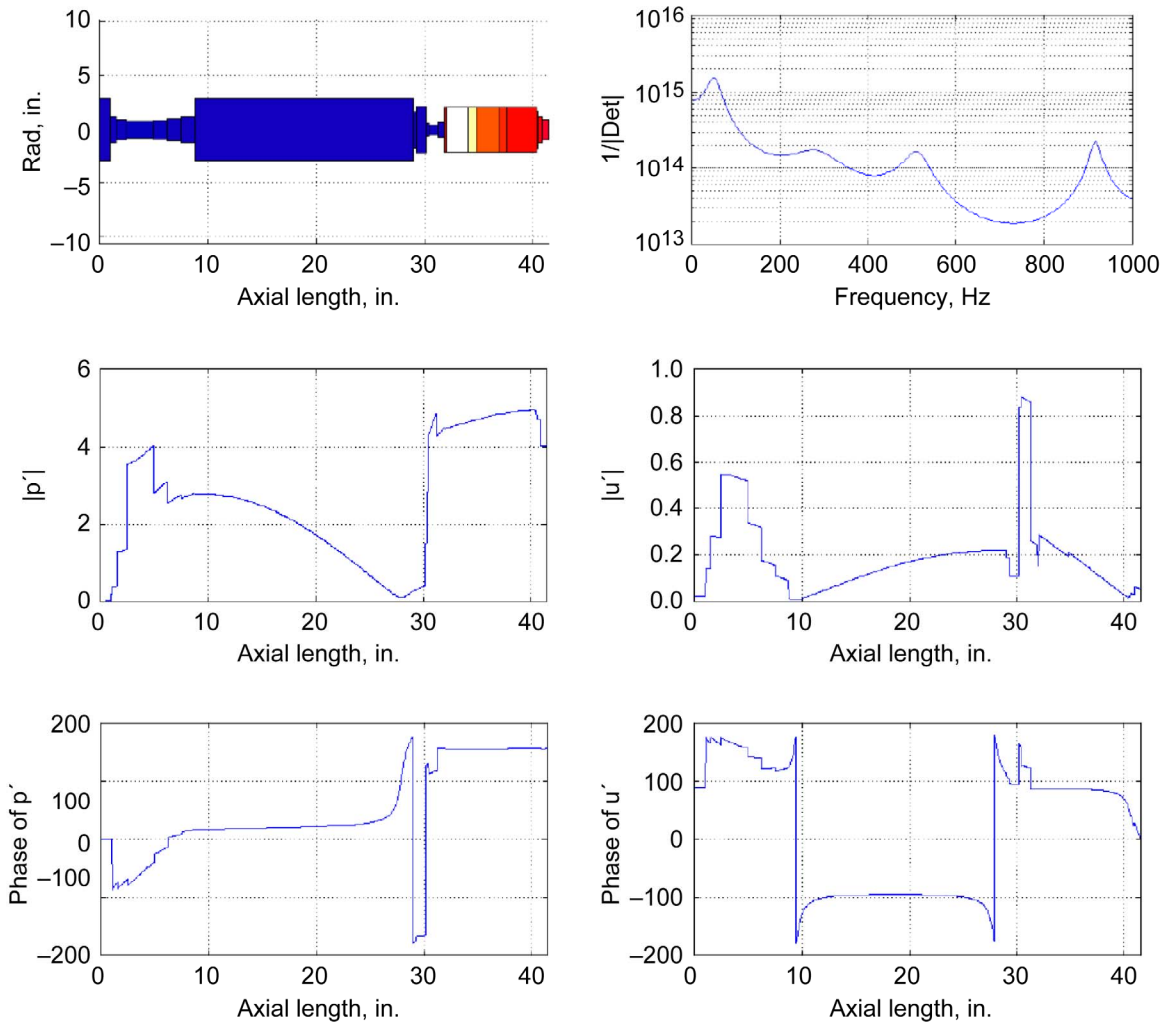

Figure 3.2.—Acoustic standing-wave predictions for the 275 Hz Mode with the 19 in. upstream extension. Amplitude and phase of the time varying pressure (p´) and velocity (u´) show the mode shape through the combustor.
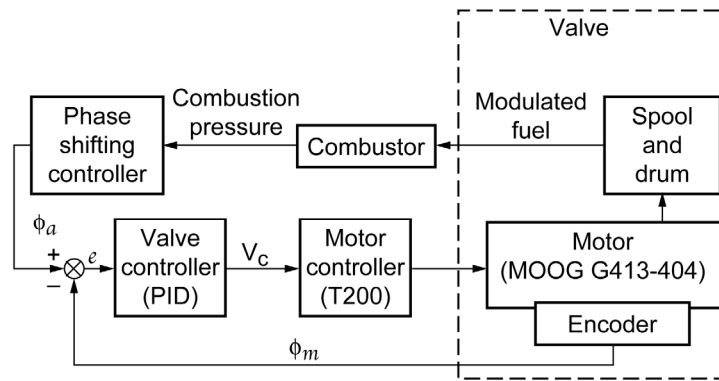
Figure 3.3.—Block diagram of the spinning valve controller.

The advantage of the frequency tracking EKF observer was that even if the main mode frequency of the oscillations changed from its nominal value, as long as the rate of change was slow, the observer kept track of the main mode frequency and the signal to noise ratio of the filtered signal was maintained. It was observed that the maximum rate of change in the peak frequency that the observer could track was about 5 Hz/s.

The spinning valve presented a unique challenge in adapting it to closed-loop control. The shaft position had to be controlled such that it followed a certain trajectory yielding the fuel modulation with a desired frequency and phase. This was done by running the motor in the 'torque mode' where the command to the motor controller controlled the motor armature current. A PID controller determined the motor control command. Figure 3.3 shows the block diagram of the spinning valve control system. V_c (command to the motor controller) was the control input and ϕ_m (shaft position) was the output. ϕ_m was measured with an encoder and had to follow a desired trajectory, which was determined from the phase of the combustor pressure.

The phase of the fuel modulation and the phase of the motor shaft were therefore related by a factor N_H (number of holes on the drum, namely 12). If the phase of the motor shaft was ϕ_m and the location of the hole nearest the 0 point of the shaft in the direction of rotation was ϕ_h, the phase of the fuel modulation measured immediately downstream of the valve would be $12\phi_m + \phi_h$. Due to the feed line and injector dynamics, the phase of the fuel modulation into the combustor was not the same as that at the outlet of the valve. If the phase difference introduced by the feed line and injector was ϕ_f, then the phase of fuel modulation into the combustor would be $12\phi_m + \phi_h + \phi_f$. For positive voltage command, the shaft always rotated in a CW direction looking from the shaft end. The direction of rotation was always kept the same by allowing only positive commands. If ϕ_c was the phase of the combustion pressure at any time, and γ was the control phase shift, the desired fuel pressure phase was $\phi_m + \gamma$. Hence the problem reduced to making $12\phi_m + \phi_h + \phi_f$ follow $\phi_m + \gamma$ as closely as possible. This was simplified to a tracking problem of ϕ_m following $(\phi_c + \gamma)/12$ as closely as possible. This simplification was possible since all the other phases are constant with time and was taken care of by the control phase γ. The phase $(\phi_c + \gamma)/12$ was the desired motor shaft phase ϕ_d.

Another issue that had to be resolved since the measured phase was between 0 and 2π was determining which ramp to track (Fig. 3.4). To get around this problem, the phase angles were added to create a single phase-ramp instead of a saw-tooth phase trajectory. However, since the phases cannot be stacked infinitely due to finite floating-point number sizes, the value eventually had to be reduced by an integral multiple of 2π in order to make it small again. Some bookkeeping had to be done at this point to ensure all variables were modified uniformly (especially the derivative of error, etc.). The result was that the desired phase trajectory was a saw-tooth function with period much larger than 2π, but an integral multiple of it (Fig. 3.5).
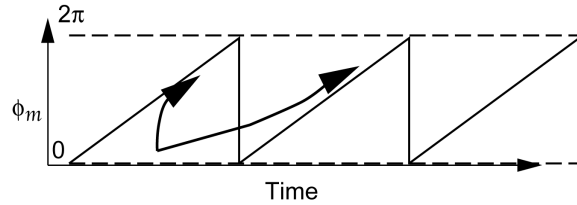
Figure 3.4.—Schematic of change in shaft positions during several cycles of rotation. This behavior led to an ambiguity in deciding which branch to track.
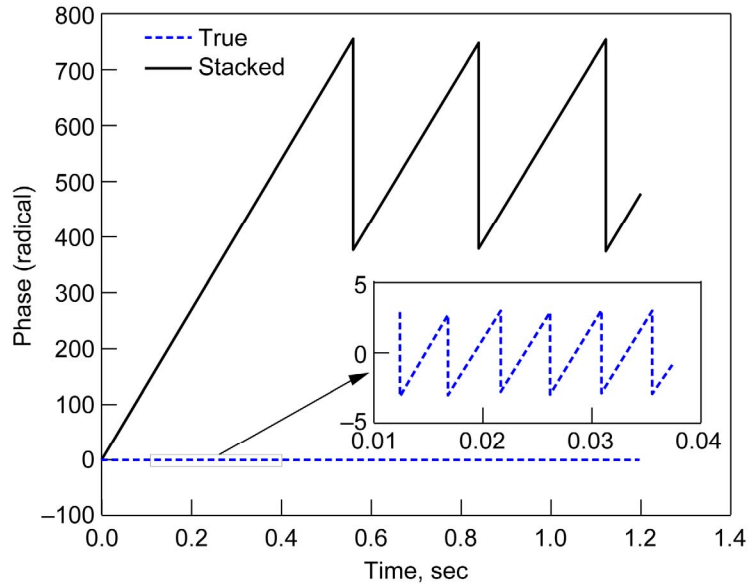

Figure 3.5.—Stacking of combustor pressure phase to create a single trajectory to follow.

An incremental 3-channel encoder measured the position of the motor shaft. The encoder was an HP HEDS 6540 three-channel encoder with a resolution of 1024 counts per revolution. The output of the circuit was the measured motor shaft position in volts (–9.89 to 9.86 V for 0 to 2π). The encoder's two quadrature outputs were used to produce the incremental position advance measurement, and the absolute position information was inferred with the help of the third index channel, which produced a high signal once per revolution – always at the same position of the codewheel.

A PID controller was used to control the motor shaft angle by commanding the required command input V_c to the spinning valve motor. It should be noted that part of the loop, from the motor shaft rotation to the fuel modulation into the combustor, was run open loop. The motor shaft position was not controlled to produce minimum error between the phase of modulated fuel in the combustor and the phase of the combustion pressure, but to minimize the error between the motor shaft position and a calculated desired position that was expected to yield a fuel modulation that follows the phase of the combustion pressure. The tracking error was defined as the desired minus the actual shaft position, $e = \phi_d - \phi_m$. The control command was compared as a combination of the error, the derivative error, and the integral of the error

$$V_c = K_p e + K_I \int_{t_o}^{t} e\,dt + K_D \frac{de}{dt} \qquad (4)$$

where the parameters K_p, K_I, and K_D are to be determined appropriately to make the shaft position follow the desired phase ϕ_d as closely as possible.

To design an effective PID controller, an accurate model of the spinning valve was needed. For a DC motor, the relation between motor armature current I_m and shaft position ϕ_m (in radians) is given by a 1st order transfer function. Since the valve is a combination of a DC motor and a spool rotating on a fluid film, its overall dynamics can be expected to be more complicated than that of just the motor.

Step input tests were done with the spinning valve where step inputs of voltage were supplied to the motor in the 'torque mode' and resulting shaft rotation was examined to identify the transfer function of the valve. Tests were done in the fuel bench under various operating conditions (i.e., different fuel system base pressures and different levels of step inputs) to investigate if there were non-linearities in the system, and if any, how strong those effects were.

Figure 3.6 shows the results of such a test (step in $V_c = +0.65$ V). The best-fit second order system to match the response of the valve was

$$G_{V2f} = \frac{0.156(z+0.687)}{(z+0.823)(z-0.991)} \tag{5}$$

with a sampling rate of 4 kHz.

Step input tests with different command steps yielded very similar results when it was a positive step. For negative steps, i.e., when the voltage command was reduced, the valve responses were considerably different from those for positive steps. The best fit transfer function for a negative step input test (step in $V_c = -0.6$ V) was

$$G_{v2f} = \frac{0.053(z-0.835)}{(z-0.941)(z-0.991)} \tag{6}$$

(4 kHz sampling rate) and was considerably different from the transfer function in equation (5).
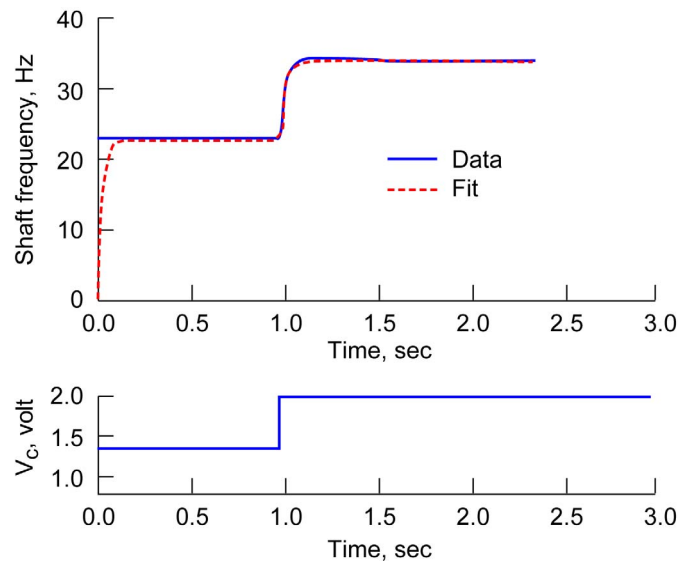

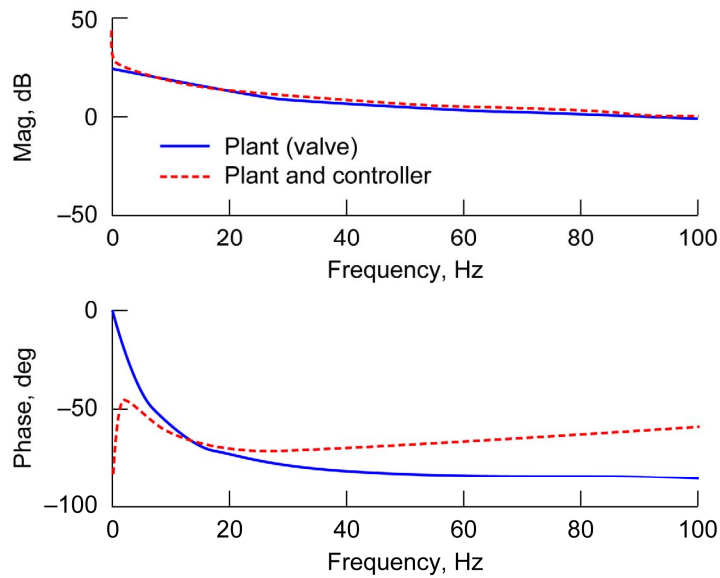Figure 3.6.—Response of the spinning valve in a step-input test.

Figure 3.7.—Bode plot of the identified valve transfer function. The transfer
function (solid blue) and loop transfer function (dashed red) which is a
product of valve and controller transfer functions G_{loop} = Gv*Gc.

The system transfer function depended on the direction of control input (commanded V_c); hence a controller designed on the basis of one such identified model would not work well under different circumstances. Hence it was decided to tune the PID gains for a nominal model to get a good phase margin with the required bandwidth; and use those values as initial guesses in real application. The PID gains were tuned during debugging of the control system by commanding the fuel modulation system to track a sinusoidal signal from an analyzer. The choice of a PID controller can itself be questioned for such a non-linear plant. PID was chosen over more sophisticated techniques due to its ease of implementation.

Figure 3.7 shows the Bode plot of the loop transfer function of the plant and controller. The plant was the spinning valve model as identified from the step response test described earlier (Eq. (5)) and the controller was the one designed according to the above procedure with a gain crossover set to 100 Hz. The PID gains were K_p = 1.1, K_I = 6.8, and K_D = 0.001. Since the fuel modulation frequency was 12 times that of the motor, the bandwidth of the system was 1200 Hz, well beyond the nominal operating point of 280 Hz for the low frequency rig configuration instability. The phase margin was about 120°.

Since the identified valve models were recognized as not very useful in representing the system, evaluating the controller's performance in simulation using these models was not useful. One point should be noted here that since the fuel modulation produced by the valve is twelve times the motor shaft frequency, small errors in the shaft position result in large errors between the commanded and actual fuel pressure phase.

3.3 NASA Developed Control Methods Used With the Georgia Tech Valve

In order to achieve closed-loop suppression of the combustion instability using the Georgia Tech magnetostrictive valve, two control methods were developed by NASA for testing at UTRC [DeLaat and Chang, 2003]. These control methods were formulated to deal with the large wideband combustor noise, severe time-delay, and randomness in phase associated with the combustor thermo-acoustic pressure oscillations.

The first control method was based on an adaptive, phase-shifting approach. This controller senses the combustion pressure, calculates the average power in the pressure oscillations, and adapts the phase of the valve-commanded fuel flow variations in order to reduce the power in the pressure oscillations. A

fast-acting phase-adaptation algorithm converges to the phase region that causes cancellation. By constantly dithering the phase within that phase region, the algorithm rapidly adapts to randomness in the instability pressure, especially that due to background combustor noise. The algorithm also provides a slower, more gradual adaptation of the controller gain. Further details on the Adaptive Sliding Phasor Averaged Control (ASPAC) method can be found in the References [Kopasakis et al., 2002, 2003].

The second control method is a model-based approach [Le et al., 2003]. This controller, like the first method, also senses combustion pressure. The method combines a "multi-scale" (wavelet like) analysis and an Extended Kalman Filter observer to predict (model) the time delayed states of the thermo-acoustic combustion pressure oscillations. The commanded fuel modulation is calculated from a predictive (damper) action based on the predicted states, and an adaptive, tone suppression action based on the multi-scale estimation of the pressure oscillations and other transient disturbances. The controller attempts to automatically adjust the gain and phase of these actions to minimize time-scale averaged variances of the combustor pressure.

4.0 Active Control Demonstration Tests

4.1 Low-Frequency Configuration—Spinning Valve with Phase-Shifting Control Method

The spinning valve with the UTRC control method was used for closed-loop combustion control with the low-frequency configuration (275 Hz mode) of the single-nozzle rig combustor. The nominal test conditions for the low-frequency mode are the mid-power conditions listed in Table 1. The experimental setup for the demonstrations is shown in Figure 4.1. Combustor pressure was sensed about 2 in. downstream of the fuel injector. The control algorithms were implemented on a dSpace real-time processor. The fuel flow was dynamically controlled via the high-response spinning valve system.

TABLE 1.—COMBUSTOR OPERATING CONDITIONS AND
UNCONTROLLED INSTABILITY CHARACTERISTICS
FOR THE LOW-FREQUENCY INSTABILITY AT 275 HZ

Test variable	Mean value
Inlet Air Pressure, P_3 (psia)	110
Inlet Air Temperature, T_3 (°F)	610
Fuel Flow Rate, W_f (lbm/hr)	207
Air Flow Rate, W_a (lbm/sec)	2.55
Unsteady Pressure Amplitude, P'_{comb} (psi)	6.5
Mean Fuel/Air Ratio	0.022
Instability Frequency (Hz)	280

The nominal operating point was established first by setting the inlet air temperature, fuel flow rate, and air flow rate. Baseline uncontrolled measurements of the instability were then acquired. Figure 4.2 shows a typical set of data, presenting a short time trace of the pressure, the corresponding amplitude spectrum (amplitude as a function of frequency) and the PDF (Probability Density Function) of the fluctuating combustion pressure, P'_{comb}.

The shape of the PDF shows this to be a limit-cycling instability according to the criteria given by [Cohen and Banaszuk, 2003]. The amplitude spectrum is computed by calculating the power spectrum with Welch's averaged periodogram method (using MATLAB's PSD function) and then using the following scaling formula to compute amplitude as a function of frequency:

$$A_p(f) = 2 * \sqrt{PSD(p') \frac{\|w\|^2}{(\sum w)^2}} \tag{7}$$

where $A_p(f)$ is the amplitude, p' is the fluctuating combustion pressure and w is a Hanning window of length equal to the number of FFT points chosen. The number of FFT points was 4096, yielding a frequency resolution of 1.2 Hz for the 5 kHz sampling rate used in data acquisition.

Closed-loop control was implemented by modulating the fuel flow rate and varying the phase shift of the control signal through a complete cycle of 360° with 30° increments and measuring combustor pressure response at those test conditions. Inlet temperature, fuel flow rate and air flow rate were held constant through the test. The PID gains used for the valve controller were $K_p = 2$, $K_I = 1$, and $K_D = 0.005$. These were empirically determined by trial and error. Figure 4.3 shows the peak amplitude of combustor pressure near 280 Hz relative to the uncontrolled level of 6.5 psi and also the RMS of P'_{comb} as a function of control phase shift. Note the amplitude could be suppressed as well as increased, depending on the control phase selected. The largest suppression of the peak amplitude (~3 times) was achieved at a control phase shift between 180° to 225°. The attenuation of the RMS value was smaller (~15 percent), and occurred at a phase shift of about 270°. Note that the RMS value was computed from the time trace data directly and the peak amplitude near 280 Hz was extracted from the amplitude spectrum calculation as explained previously.
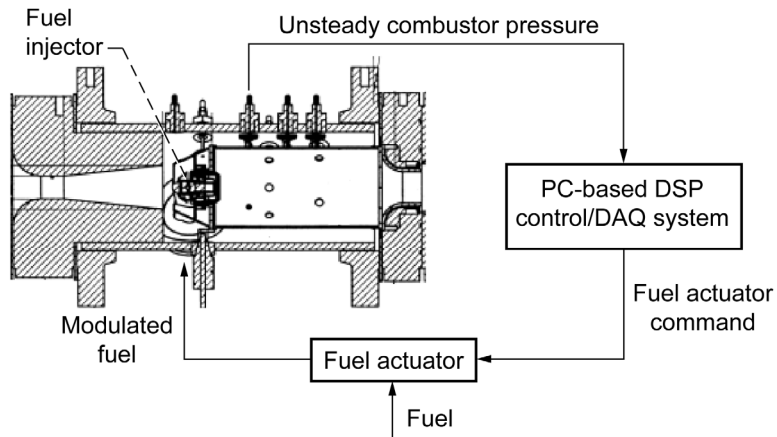
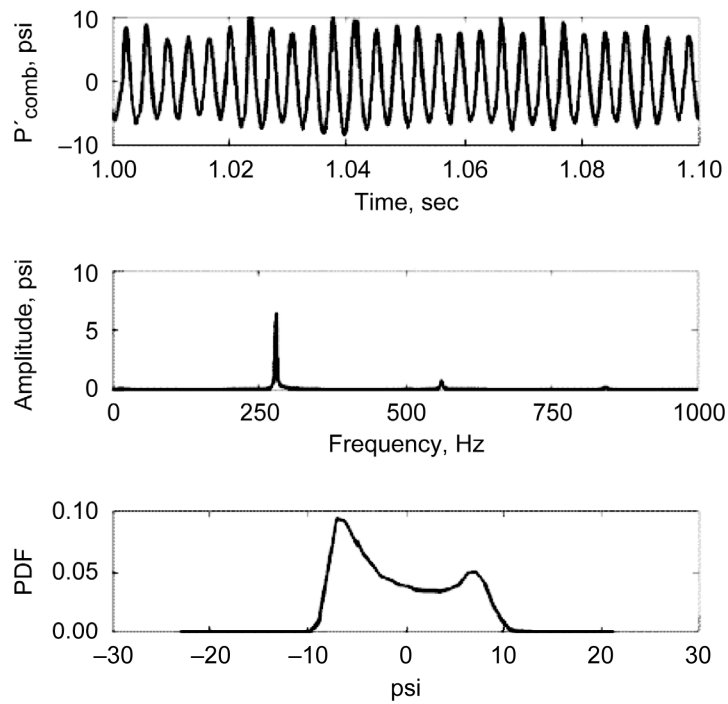Figure 4.1.—Single-nozzle rig setup for combustion control experiments.

Figure 4.2.—Typical instability characteristics for the low-frequency 275 Hz mode. Time trace, amplitude spectrum, and PDF of fluctuating pressure in the 280 Hz instability condition (mid-power).
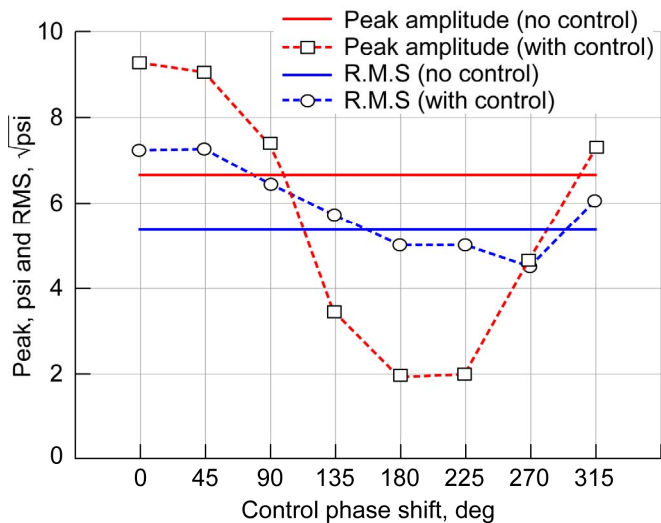
Figure 4.3.—Peak amplitude near 280 Hz and RMS value of combustor pressure as a function of control phase. Shows difference between amplitude and RMS attenuation.
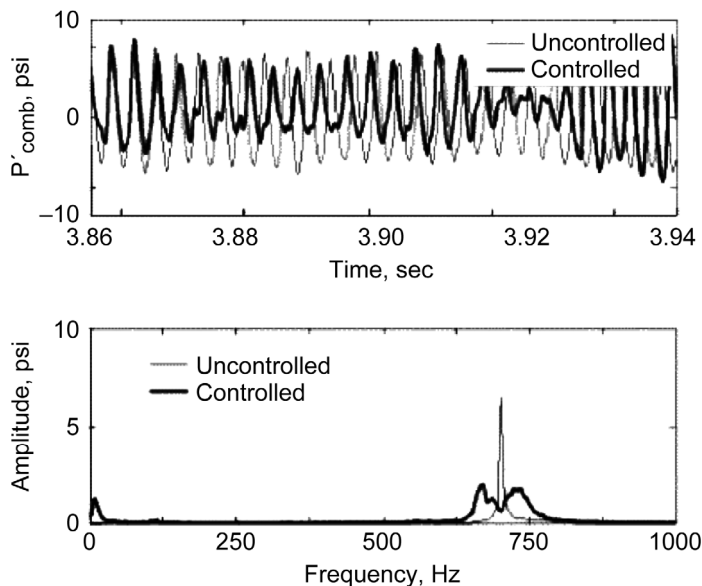

Figure 4.4.—Comparison of combustion pressure amplitude spectra for uncontrolled and the best controlled point.

Figure 4.4 shows a comparison of the uncontrolled and controlled amplitude spectra of the fluctuating combustor pressure for the point where best attenuation was achieved. The amplitude at the instability frequency (280 Hz) was reduced by a factor of 10, but side-lobes are evident. The time traces show that during control, oscillations were not uniformly low over time. A 'peak-splitting' phenomenon occurs resulting in oscillations above and below the uncontrolled frequency. Peak-splitting [Cohen and Banaszuk, 2003], which has been observed in many other active combustion instability control demonstrations, was the primary reason why attenuation of the RMS was considerably less than that for the tonal peak.

Control authority in this case may also have been affected by the tracking performance of the spinning valve controller. Figure 4.5 shows the difference between the instantaneous phases of the combustion pressure and the fuel pressure (measured downstream of the valve) for the best-controlled case. The commanded control phase shift was constant, so the valve should modulate fuel with a constant phase difference from the combustor pressure. However, Figure 4.5 shows that the valve periodically lost tracking by as much as 250°. It was found that this periodic change in the phase difference between combustor and fuel line pressures was due to the loss of tracking by the spinning valve motor. Since the spinning valve drum had 12 holes, the fuel modulation frequency was 12 times the motor shaft frequency. Therefore the difference between fuel pressure phase and $12\phi_m$ should be constant. Figure 4.6 shows the difference between the fuel line pressure (downstream of valve) and $12\phi_m$. The phase difference was not constant, but was slowly drifting in one direction. This could have been caused by one of two things: either the shaft encoder code-wheel was slipping on the motor shaft, or the encoder electronics were not measuring the position accurately. Unfortunately, none of these hypotheses can be checked with available data. This 'phase drift' likely contributed to the poor control performance.
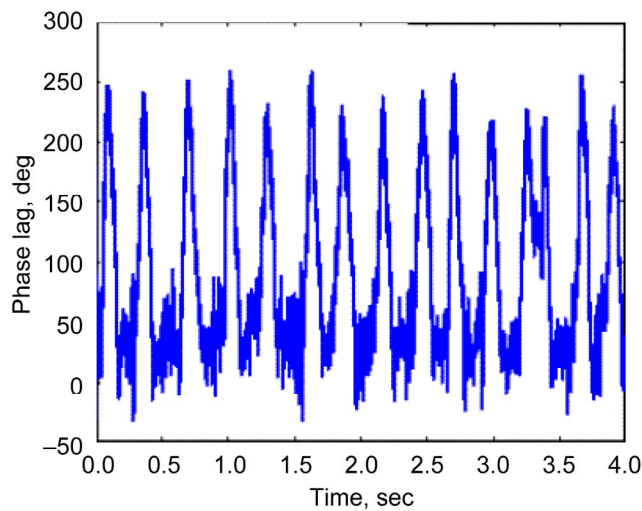
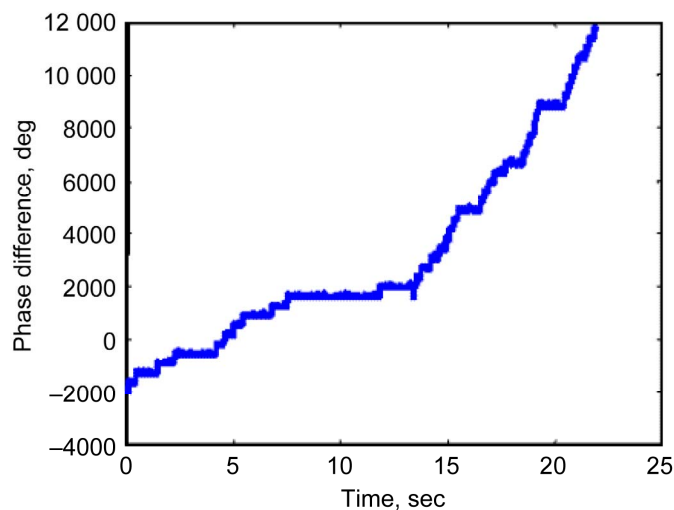Figure 4.5.—Instantaneous phase difference between P_{fuel} and P'_{comb} during closed loop control.

Figure 4.6.—Instantaneous difference between the phase of fuel pressure and 12*(motor shaft position).

4.2 Low-Frequency Configuration—Moog DDV Valve

Tests with the Moog direct drive valve (DDV) were conducted to evaluate the control capability with the DDV operating in a proportional manner, where fuel modulation amplitude was a control parameter. This valve could allow the importance of valve bandwidth and modulation strength to be examined. However, both the flow bench results (see Section 2.4) and the combustion tests demonstrated that the dynamics of the fuel feed system with the valve operating in proportional mode had a limited ability to control the fuel flow history.

Unforced and open-loop forcing tests were conducted at the beginning of the run to characterize the combustor and actuator. Closed-loop testing followed with the valve, operating in a proportional mode, being commanded by a phase-shift control method. Effective control was not observed in that test. The limits on valve travel were changed to allow the valve to operate in a full on/off mode. The combustion test results showed that the valve was less effective operating proportionally and more effective in an on/off operating regime. A final set of test runs using the valve in the on/off mode at the mid-power condition showed, as in earlier tests, that the spectral peak of the instability was lowered by a factor of about 3 in closed-loop tests but the spectral width was broadened with significant peak-splitting so that the energy was not significantly diminished. An example of the test results using the Moog DDV valve are shown in Figure 4.7.
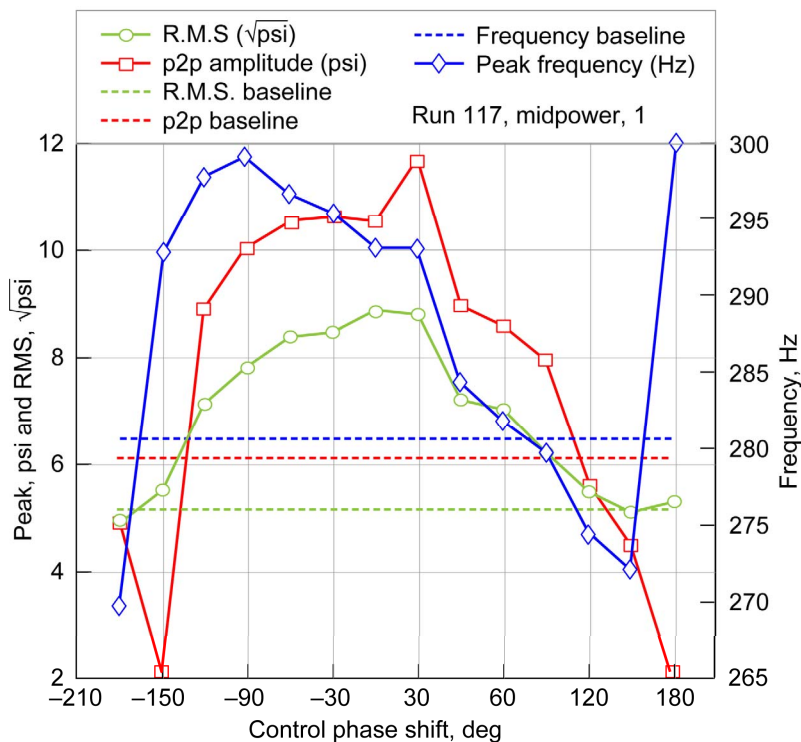

Figure 4.7.—Peak amplitude near 280 Hz and RMS value of combustor pressure as a function of control phase using the Moog DDV valve in on-off mode as compared to the no control (baseline) case.

4.3 High-Frequency Configuration—Georgia Tech Valve With NASA-Developed Control Methods

In the next phase of the program, the Georgia Tech valve and the two NASA-developed control methods were employed to investigate closed-loop combustion control of the high frequency mode (530 Hz) in the single-nozzle rig combustor. The rig was operated at the high-power conditions shown in Table 2 and configured to produce a 530 Hz instability. The fuel flow for this set of tests was higher than for the Phase I testing and was chosen empirically to maximize the instability. The typical uncontrolled instability behavior is shown in Figure 4.8. It can be seen that this instability at 530 Hz differs from the low-frequency instability at 280 Hz in that it is not limit cycling and the amplitude is much weaker. The Gaussian distribution of the PDF indicates a noise-driven, stable oscillating system.

TABLE 2.—COMBUSTOR OPERATING CONDITIONS AND
UNCONTROLLED INSTABILITY CHARACTERISTICS
FOR THE HIGH-FREQUENCY INSTABILITY

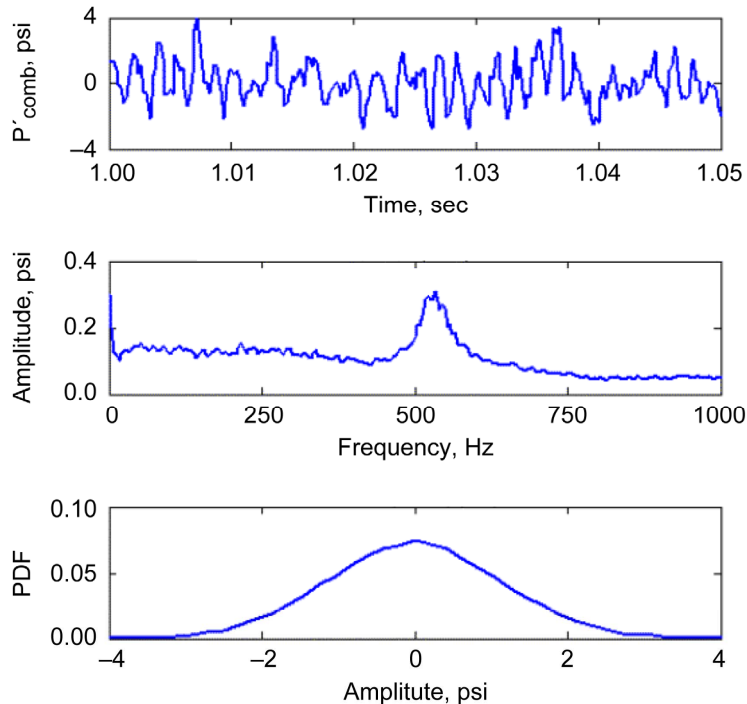| Test variable	Mean value
Inlet Air Pressure, P_3 (psia)	175
Inlet Air Temperature, T_3 (°F)	775
Fuel Flow Rate, W_f (lbm/hr)	450
Air Flow Rate, W_a (lbm/sec)	3.4
Unsteady Pressure Amplitude, P'_{comb} (psi)	0.3
Mean Fuel/Air Ratio	0.038
Instability Frequency (Hz)	530

Figure 4.8.—Typical instability characteristics for the high-frequency
mode. Time trace, amplitude spectrum, and PDF of fluctuating
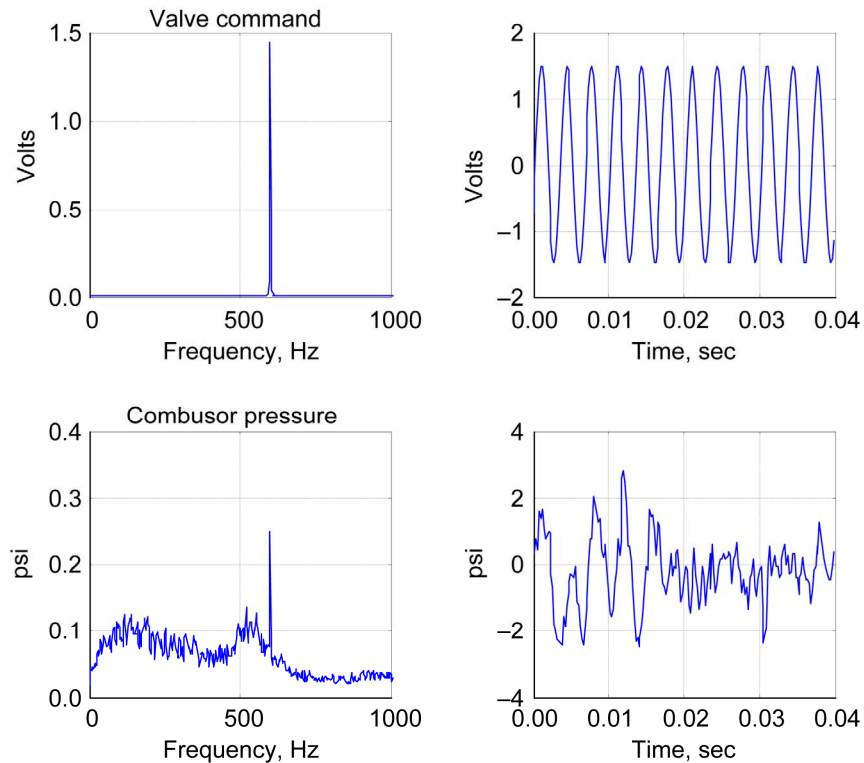combustor pressure in the 530 Hz instability condition (high-power).

Figure 4.9.—Unsteady combustor pressure amplitude response to a valve
perturbation command of ±1.5 V at 600 Hz.

For the evaluation of each controller, the baseline operating condition was established first. The fuel was then modulated open loop in order to verify the operation of the actuator and the level of authority. A typical example is shown in Figure 4.9 for a 600 Hz valve perturbation. Next, the closed-loop controller was implemented. Two sets of experiments were run with both controllers being evaluated each time. During the first test, a significant reduction in instability amplitude was observed for both control methods as shown in Figure 4.10. However, for both control methods, a low frequency (<30 Hz) oscillation was seen in the combustor pressure frequency spectrum, particularly with the model-based controller. It was suspected that these low frequency oscillations were due to interactions between the instability control at high frequency and the valve mean-flow control occurring at low frequency. Note that with these control methods and the relatively low instability level, the peak-splitting phenomena did not appear to be generated.

For the second set of tests, additional filtering was added to the controllers to reduce this low-frequency interaction. The results, shown in Figure 4.11, demonstrate that this approach was effective in eliminating the low frequency oscillations. More importantly, both control methods were able to identify the instability frequency and reduce the amplitude by approximately 30 percent. This was accomplished without inducing the peak-splitting phenomena, or sideband peaks, as was observed in the low-frequency combustion instability control studies previously discussed.
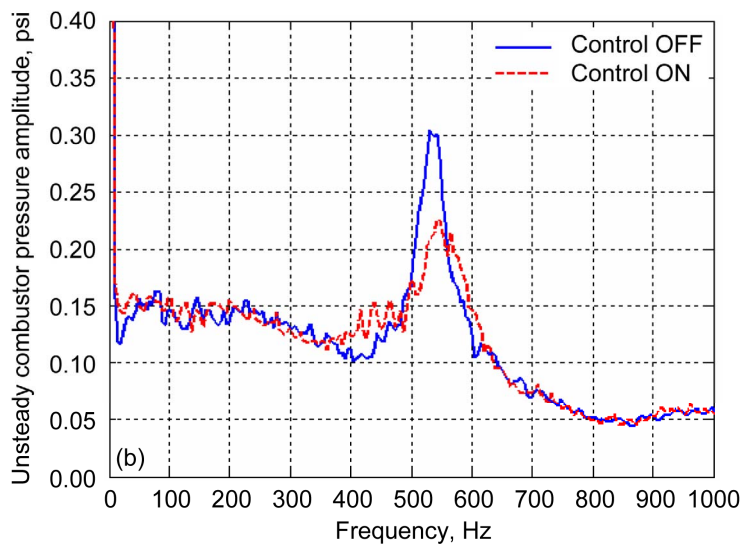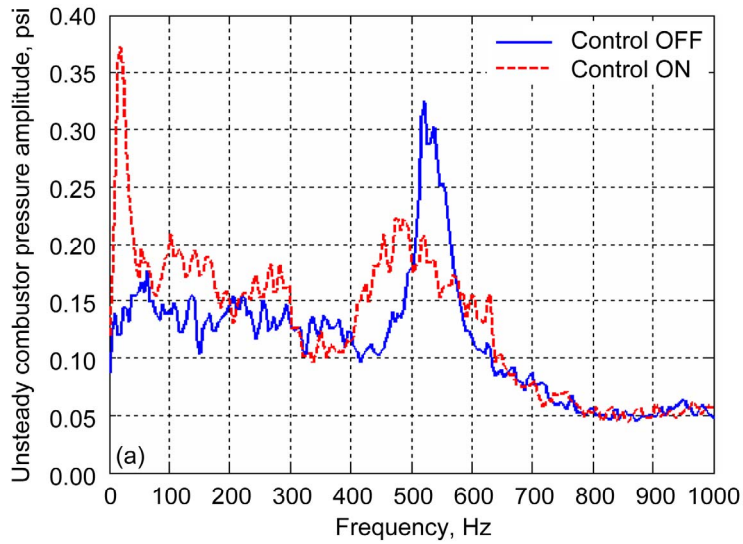
Figure 4.10.—Initial set of experiments showing unsteady combustor pressure amplitude spectra for high-frequency control. For (a) model-based control method and (b) adaptive phase-shifting control method.
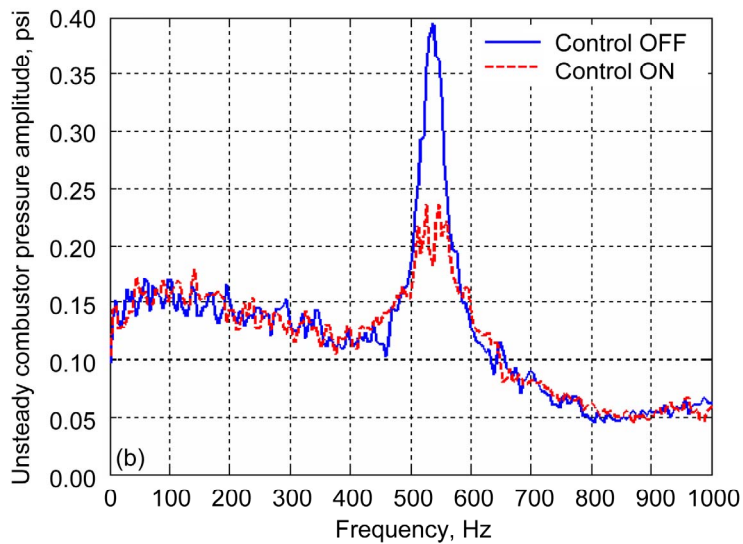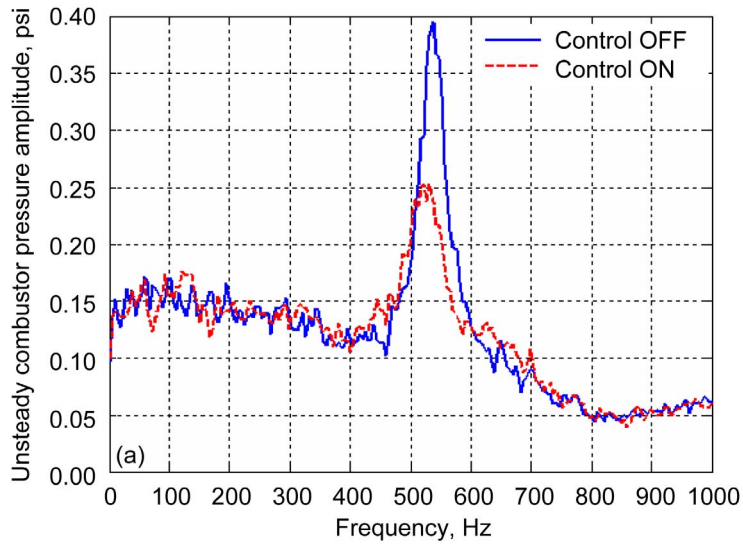
Figure 4.11.—Second set of experiments showing unsteady combustor pressure amplitude spectra for high-frequency control. For (a) model-based control method and (b) adaptive phase-shifting control method. Both control methods show improved performance over the initial set of experiments.

5.0 Summary and Discussion

The primary objective of this NASA sponsored program was to demonstrate the potential of active combustion instability control using an engine-traceable test platform. This program successfully demonstrated this objective and provided substantial insight into the issues and challenges for this technology.

The Phase I effort identified a candidate engine instability and developed a single-nozzle test rig to successfully replicate the instability. This effort demonstrated that if the acoustic boundary conditions are faithfully replicated and if controlling parameters such as the sub-component lengths, cross-sectional area distribution, flow distribution, pressure-drop distribution and temperature distribution are also replicated, then an instability can be reproduced in a rig environment that is essentially of the same origin as in the engine. The baseline test configuration demonstrated a high-frequency longitudinal combustion instability at 570 Hz that was similar to that observed in a P&W technology demonstrator engine using the specific tri-wall swirler fuel nozzle. In addition, a long 19 in. spool section could be installed upstream of the combustor to produce a much stronger amplitude instability at 270 Hz. Acoustic modeling validated that this mode was associated with a half-wave longitudinal standing wave.

The goal of the Phase II effort, the subject of this report, was to employ a fuel-modulation based feedback-control system to demonstrate active combustion control. The availability of a high-frequency fuel actuator valve that can provide adequate and reliable fuel modulation remains one of the primary challenges for this technology. Previous laboratory experiments indicated that a heat release modulation strength of at least 5 to 10 percent is needed to affect combustion instabilities. Significant attenuation of the fuel modulation is anticipated from the fuel injection and mixing processes; therefore, the fuel actuation system must likely be capable of producing very large fuel flow modulation to ultimately provide sufficient control authority for the instability. Significant efforts were expended in the current effort to better understand these aspects of the active control system.

A spinning-valve fuel actuator developed at UTRC demonstrated the ability to generate very large fuel flow modulation and so provided one option to modulate the fuel in the active control system. Bench tests measuring the fluctuating fuel pressure indicated that a fuel flow modulation of about 60 percent could be generated with the valve out to about 450 Hz. Imaging methods were developed which appear to confirm the 60 percent modulation level. Laser extinction methods were then developed to obtain a measure of the fuel modulation in the presence of the swirler air stream and these measurements indicated that the fuel modulation at 570 Hz was attenuated by about 8x by the injection and mixing processes. The spinning valve was initially used for open-loop modulation of the fuel into the combustor rig configured for the 275 Hz low-frequency mode, and then to demonstrate active control for this rig configuration. The valve produced a modulation strength of about 60 percent and estimated fuel modulation at the flame of 10 percent.

A Moog DDV valve was also investigated briefly as a source for active control with the potential to use this valve as a proportional valve. Bench testing and combustor testing showed that significant acoustic resonance occurred in the fuel system using this valve precluding the use of this valve in a proportional mode.

A high-frequency fuel actuator, developed at Georgia Tech and based on magnetostrictive technology, was also characterized and was found to be capable of generating fuel modulation above 30 percent out to frequencies over 700 Hz. This valve was initially used for open-loop modulation of the fuel into the combustor rig configured for the 570 Hz high-frequency mode, and then to demonstrate active control for this rig configuration. The valve produced a modulation strength of about 40 percent and estimated fuel modulation at the flame of 4 percent.

Active instability control was first demonstrated on a fairly strong 275 Hz instability using the spinning-valve fuel actuator and a phase-shifting controller. The pressure oscillations at 275 Hz were reduced by an order of magnitude, but significant peak-splitting of the energy into side lobes in the frequency domain resulted in only about a 15 percent reduction in the root-mean-square of the pressure

fluctuations. The difficulty of phase-synchronizing the spinning valve to the varying phase of the pressure oscillations may have reduced the controller's effectiveness. One active control run was also made using the Moog DDV valve which showed similar effectiveness on the 275 Hz mode, but again with significant peak-splitting of the energy when using a simple phase shift controller.

A second demonstration of active control was accomplished with the combustor rig configured for the weaker, engine-traceable 570 Hz instability using the high-frequency magnetostrictive fuel actuator. Advanced control algorithms were developed by NASA Glenn to try to minimize the peak splitting behavior seen in all the other control demonstrations. Instability suppression was successfully demonstrated using both model-based and adaptive control algorithms developed by NASA-GRC. These control methods reduced the pressure amplitude about 30 percent and showed no signs of the peak-splitting phenomena.

6.0 Conclusions

The results of this program clearly demonstrate the potential of active instability control using fuel modulation for aircraft gas turbine main combustors. The test rig developed for this program included all the features that can limit the effectiveness of active control, such as an air-assist fuel nozzle, wall cooling and strong recirculation zones. Significant control authority was demonstrated by modulating the fuel to the main fuel injector with no modifications. Several fuel actuator concepts were demonstrated as were three different control algorithms. The results show that a significant reduction in oscillation amplitude can be achieved using a simple phase shifting controller, but "peak-splitting" occurs and energy is redirected into side frequencies resulting in only a small reduction in the power of unsteady oscillations. The results of this study show that advanced control methods can potentially eliminate "peak-splitting" and improve the suppression effectiveness, reducing the oscillation power levels. The results of bench tests developed to quantify the fuel modulation achieved, and observations during experimental testing of active control indicate that modulation authority of about 10 percent may be sufficient to couple with the combustion processes and provide significant suppression of the instability. The results of this work show that, with some development for the particular application to increase effectiveness and authority, active control is a viable approach for mitigating combustion instabilities for low and high frequency instabilities in aircraft engine combustion systems.

References

Anderson, T.J., Kendrick, D.W., and Cohen, J.M., 1998: "Measurement of Spray/Acoustic Coupling in Gas Turbine Fuel Injectors," AIAA Paper 98-0718, Reno NV.

Banaszuk, A., Jacobson, C.A., Khibnik, A.I., and Mehta, P.G. 1999: "Linear and Nonlinear Analysis of Controlled Combustion Processes. Part I: Linear Analysis," Proceedings of the 1999 IEEE International Conference on Control Applications, vol. 1, pp. 199–205.

Billoud, G., Galland, M.A., Huynh Huu, C., and Candel, S., 1992: "Adaptive Active Control of Combustion Instabilities," Combustion Science and Technology, vol. 81, issue 4, pp. 257–283.

Cohen, J.M, et al., 2000: "Experimental Replication of an Aeroengine Combustion Instability," ASME International Gas Turbine and Aeroengine Technical Congress, Munich, Germany, NASA/TM—2000-210250, ASME Paper 2000–GT–0093.

Cohen, J.M., Rey, N.M., Jacobson, C.A., and Anderson, T.J., 1998: "Active Control of Combustion Instability in a Liquid-Fueled Low-NOX Combustor," ASME Paper 98–GT–267.

Cohen, J. M. and Banaszuk, A., 2003: "Factors Affecting the Control of Unstable Combustors," *Journal of Propulsion and Power,* vol. 19, no. 5, pp. 811–821.

DeLaat, J.C., Breisacher, K.J., Saus, J.R., Paxson, D.E., 2000: "Active Combustion Control for Aircraft Gas Turbine Engines," 36th Joint Propulsion Conference and Exposition, Huntsville, AL, NASA/TM—2000-210346, AIAA–2000–3500.

DeLaat, J.C.; Chang, C.T, 2003: "Active Control of High Frequency Combustion Instability in Aircraft Gas-Turbine Engines, 16th International Symposium on Airbreathing Engines, Cleveland, OH. NASA/TM—2003-212611, ISABE–2003–1054.

Hibshman, J.R., Cohen, J.M., Banaszuk, A., Anderson, T.J., and Alholm, H.A., 1999: "Active Control of Combustion Instability in a Liquid-Fueled Sector Combustor," ASME, International Gas Turbine and Aeroengine Congress and Exhibition, Indianapolis, IN,. ASME Paper 99–GT–215.

Kopasakis, G. and DeLaat, J., 2002: "Adaptive Instability Suppression Controls in a Liquid-Fueled Combustor," 38th Joint Propulsion Conference and Exhibit, Indianapolis, IN, AIAA–2002–4075, NASA/TM—2002-21805.

Kopasakis, G., 2003: "High-Frequency Instability Suppression Controls in a Liquid-Fueled Combustor", 39th Joint Propulsion Conference and Exhibit, Huntsville, AL. AIAA–2003–1458.

LaScala, B., 1994: "Approaches to Frequency Tracking and Vibration Control," Ph.D. Thesis, Dept. of Systems Engineering, The Australian National University.

Le, D., DeLaat, J., and Chang, C., 2003: "Control of Thermo-Acoustic Instabilities: The Multi-Scale Extended Kalman Approach," 39th Joint Propulsion Conference and Exhibit, Huntsville, AL. AIAA–2003–4934.

Peracchio, A., Rosfjord, T.J., McVey, J.B., et al., 1998: "Active Combustion Control for Marine and Land-Based Aeroderivative Gas Turbine Engines, DARPA Contract MDA972-95-C-0009, UTRC Report 98–16.

Peracchio, A.A. and Proscia, W., 1998: "Nonlinear Heat-Release/Acoustic Model for Thermoacoustic Instability in Lean Premixed Combustors," presented at the ASME IGTI Turbo Expo.

Zinn, B.T., and Neumeier, Y., 1997: "An Overview of Active Control of Combustion Instabilities," AIAA–97–0461.

REPORT DOCUMENTATION PAGE

1. REPORT DATE (DD-MM-YYYY)	2. REPORT TYPE	3. DATES COVERED (From - To)
01-12-2008	Final Contractor Report	

4. TITLE AND SUBTITLE
Demonstration of Active Combustion Control

5a. CONTRACT NUMBER
NAS3-98005

5b. GRANT NUMBER

5c. PROGRAM ELEMENT NUMBER

6. AUTHOR(S)
Lovett, Jeffery, A.; Teerlinck, Karen, A.; Cohen, Jeffrey, M.

5d. PROJECT NUMBER

5e. TASK NUMBER

5f. WORK UNIT NUMBER
WBS-984754.02.07.03.19.04

7. PERFORMING ORGANIZATION NAME(S) AND ADDRESS(ES)
Pratt & Whitney
East Hartford, Connecticut

8. PERFORMING ORGANIZATION REPORT NUMBER
E-16813

9. SPONSORING/MONITORING AGENCY NAME(S) AND ADDRESS(ES)
National Aeronautics and Space Administration
Washington, DC 20546-0001

10. SPONSORING/MONITORS ACRONYM(S)
NASA

11. SPONSORING/MONITORING REPORT NUMBER
NASA/CR-2008-215491

12. DISTRIBUTION/AVAILABILITY STATEMENT
Unclassified-Unlimited
Subject Category: 07
Available electronically at http://gltrs.grc.nasa.gov
This publication is available from the NASA Center for AeroSpace Information, 301-621-0390

13. SUPPLEMENTARY NOTES

14. ABSTRACT
The primary objective of this effort was to demonstrate active control of combustion instabilities in a direct-injection gas turbine combustor that accurately simulates engine operating conditions and reproduces an engine-type instability. This report documents the second phase of a two-phase effort. The first phase involved the analysis of an instability observed in a developmental aeroengine and the design of a single-nozzle test rig to replicate that phenomenon. This was successfully completed in 2001 and is documented in the Phase I report. This second phase was directed toward demonstration of active control strategies to mitigate this instability and thereby demonstrate the viability of active control for aircraft engine combustors. This involved development of high-speed actuator technology, testing and analysis of how the actuation system was integrated with the combustion system, control algorithm development, and demonstration testing in the single-nozzle test rig. A 30 percent reduction in the amplitude of the high-frequency (570 Hz) instability was achieved using actuation systems and control algorithms developed within this effort. Even larger reductions were shown with a low-frequency (270 Hz) instability. This represents a unique achievement in the development and practical demonstration of active combustion control systems for gas turbine applications.

15. SUBJECT TERMS
Aircraft engines; Combustion stability; Combustion control; Engine control

16. SECURITY CLASSIFICATION OF:			17. LIMITATION OF ABSTRACT	18. NUMBER OF PAGES	19a. NAME OF RESPONSIBLE PERSON STI Help Desk (email:help@sti.nasa.gov)
a. REPORT	b. ABSTRACT	c. THIS PAGE	UU	48	19b. TELEPHONE NUMBER (include area code)
U	U	U			301-621-0390